Published in 'Tribology International 44 (2011) 1902–1919'

Studies of High Temperature Sliding Wear of Metallic Dissimilar Interfaces IV: Nimonic 80A versus Incoloy 800HT

I.A. Inman [*], P.S. Datta [a]

a Northumbria University, Newcastle upon Tyne, NE1 8ST, UK

Abstract

Wear variations of Nimonic 80A slid against Incoloy 800HT between room temperature (R.T.) and 750°C, and sliding speeds of 0.314 and 0.905 $m.s^{-1}$ were investigated using a 'reciprocating-block-on-cylinder', low debris retention configuration. These were considered alongside previous observations at 0.654 $m.s^{-1}$.

Different wear types occurring were mapped, including high transfer 'severe wear' (R.T. and 270°C, also 0.905 $m.s^{-1}$ at ≤570°C), low transfer 'severe wear' (0.314 $m.s^{-1}$ at 390°C to 510°C – oxide abrasion assisted at 510°C), and 'mild wear' (0.314 $m.s^{-1}$ at ≥570°C; 0.905 $m.s^{-1}$ at ≥630°C). Wear surfaces at 750°C were cross-sectioned and profiled.

Keywords: high temperature; sliding speed; dissimilar materials; wear map

1. Introduction

High temperature wear is a serious problem affecting many applications such as power generation, transport, materials processing and turbine engines [1-7]. The combined action of temperature and tribological parameters accentuate the wear problem due to, for example, reductions of mechanical hardness and strength of contacting surfaces, greater rates of surface oxidation and changes in adhesion between such surfaces. The use of coatings, preoxidised surfaces, and thermally stable and oxidation resistant materials, have been used to reduce such wear [1, 5, 6, 8-12]. However, environmental conditions can severely reduce possible materials and coatings options [1-6].

Another approach for generating wear resistant surfaces is to take advantage of some of the phenomena accompanying high temperature wear, such as oxidation, debris generation and elemental transfer between contacting surfaces [1-7, 13]. Under certain favourable conditions of temperature (i.e. high), pressure / load and speed, these events lead to the generation of 'glazes' on the contacting surfaces (either two metallic or a metallic surface versus a suitable ceramic surface) that can enhance resistance to further wear [1-33]. Where such favourable conditions exist, protective 'glaze' layer formation is suggested due to a combination of elemental transfer (notably with dissimilar interface systems) and debris generation, oxidation, and sintering [1,2,4,7]. Moreover, debris' sinterability and thus the ease with which the 'glaze' is formed can be strongly affected by oxide chemistry [1,7,23,25].

So [26,27], Welsh [28,29], Lancaster [30], and others [31,32] have shown that different combinations of temperature, sliding speed and load can significantly influence wear behaviour, and whether or not a protective 'glaze' forms. Some authors have constructed sliding wear maps to try to present such wear data in an easily understood format, facilitating prediction of probable wear mode under specific sliding conditions. Examples of wear map parameters used include load / pressure versus sliding speed [34-44], 'severity of contact' and 'thermal severity of contact' with ceramic wear [45] and even 'degree of penetration (of asperities)' and 'shear strength at the contact

* Corresponding author - *E-mail address:* ian@tibet.freeserve.co.uk (I.A. Inman).

interface' [46]. However, most wear maps use room temperature (R.T.) data with little work at elevated temperature (an exception is Gómez-del Río et al [44]) or using dissimilar interfaces.

Examination of Incoloy MA 956 [23,25] or Nimonic 80A [1,4,6,7,24] versus Stellite 6, or Incoloy MA956 versus Incoloy 800HT [1,25] (all 'dissimilar interface' sliding systems) has shown that temperature in combination with sliding speed can affect the observed wear mode and also the material likely to undergo greater wear. In all three cases, simple 'temperature versus sliding speed' wear maps were created from the collected data [7,23-25].

Additionally, the wear resistance of many Co-based alloys such as Stellite 6 is already well understood [1-7, 23, 24, 26, 47-51]. This resistance is due partially to a tendency to undergo a shear-induced 'face-centred cubic' to 'hexagonal-close-packed' structural transformation [47-49]. A thin, easily sheared layer can develop at the sliding surface promoting easy glide, due to shear-induced alignment of the 'hexagonal-close-packed' basal plane parallel to sliding direction [49,50]. This alignment significantly improves galling resistance and reduces friction, with shear and adhesive transfer restricted to this layer; this sliding regime continues even after layer removal due to ready regeneration of the layer. Additionally, material removal in such thin sections can partially explain ready generation of fine Stellite 6-sourced Co-based oxide debris observed in previous studies [1,2,5-7,23,24,51], as they may be commutable to a small size and more easily oxidised to provide a ready material supply notably for high temperature wear-protective 'glaze' layer formation.

In contrast, both 'face-centred cubic' (Incoloy 800HT and Nimonic 80A) and 'body-centred cubic' (Incoloy MA956) systems have 12 primary slip systems available compared to 3 basal plane slip systems for 'hexagonal-close-packed' alloys [52,53]. Furthermore, the number of active slip systems in 'body-centred cubic' structures may be increased by raising temperature [52] or shear stress [53]; slip may occur on a further 36 systems with an extra 10% shear stress [53]. Such alloys thus normally have poor galling resistance compared to cobalt-based alloys. Heavy deformation and metallic debris generation (i.e. severe wear) can be expected [47] and there is potential for mechanical alloying where metallic debris from both sliding surfaces is mixed together and redeposited on either or both wear surfaces [54-56].

Such wear was observed for the Incoloy MA956 versus Incoloy 800HT (counterface) wear pair [1,25]. The presence of a second phase in both alloys [57,58] normally used to improve mechanical and high temperature properties, showed no evidence of improving wear resistance to a useful level [25]; it is possible the high wear of 'body-centred cubic' Incoloy MA956 at high temperature may be attributable to extra slip planes becoming operational. Also, although 'glaze' formation reduced high temperature wear, this was not to acceptable levels due to continuing early 'severe wear' [25].

The current Nimonic 80A versus Incoloy 800HT (counterface) study follows on from that of Incoloy MA956 versus Incoloy 800HT by substituting 'body-centred cubic' Incoloy MA956 with

'face-centred cubic' Nimonic 80A, which possesses greater R.T. and hot hardness than Incoloy MA956 [6]. Questions to be answered include whether or not Nimonic 80A's enhanced mechanical properties are sufficient to provide greater wear resistance against the Incoloy 800HT counterface or whether microstructural considerations will once again take precedence. It is also queried whether the Fe from the Ni-Cr-Fe-based Incoloy 800HT may help produce a more sinterable oxide with greater 'glaze' forming tendency, than say the Ni- and Cr-based oxides generated from Nimonic 80A when slid against Stellite 6 at higher sliding speeds and temperatures [1,4,23].

EDX profiling of surface layers generated on Nimonic 80A slid against Incoloy 800HT (at 750°C, and sliding speeds of 0.314 and 0.905 $m.s^{-1}$), is used to establish a probable order of deformation and layer-formation events from early sliding through to final 'glaze' layer generation.

2. Experimental

2.1 Temperature versus Sliding Speed Study

The alloy compositions used in this study are detailed in Table 1. There are two sets of data for Nimonic 80A, manufacturer specified and EDX measured. It is uncertain why the supplied material composition differs from that specified (higher Cr, lower Ni and slightly higher Al and Si), however, XRD indicated only 'face-centred cubic' phase; there was a risk high Cr might introduce some 'body-centred cubic' phase. Discussion of reported data is in relation to the EDX-measured results.

The tests were carried out using a high temperature 'reciprocating-block-on-rotating-cylinder' wear rig (Nimonic 80A 'blocks' forming the samples and an Incoloy 800HT cylinder, the 'counterface') in air (Fig. 1), a configuration developed for accelerated simulation testing of car engine 'valve-on-valve-seat' wear; this matches previous methodology [1-7,23-25], redescribed for clarity and completeness. The configuration used was such that debris retention was not encouraged. The counterface, diameter 50 mm and length 50 mm, was mounted on a variable-speed-electric-motor-rotated shaft. Individual 'block' samples, 5 x 5x 45 mm (polished to a 1 µm surface finish then acetone cleaned) were held against the counterface (polished to a 1200 grit finish then acetone cleaned), using a sample arm in reciprocating motion (constant stroke 12 mm, 3 cycles per minute). The tests were carried out at sliding speeds of 0.314 and 0.905 $m.s^{-1}$, at R.T., 270, 390, 450, 510, 570, 630, 690 and 750°C under 7N load, the high temperatures achieved using a custom electrical furnace. The total sliding distance for all tests combinations was 4,522 m. 0.905 $m.s^{-1}$ tests were also conducted up to 13,032 m, to observe any changes in behaviour after extended sliding.

A minimum of three tests (one per sample) were conducted for each combination of conditions. Each Nimonic 80A sample was weighed before and after sliding using a high accuracy Sartorius microbalance, from which each set of sliding conditions' mean weight change was calculated; weight loss was recorded as a negative value. The coefficient of friction data were collected by a Melbourne type TRP-50 torque transducer connected to the rotating counterface shaft.

The microstructures at 0.314 and 0.905 $m.s^{-1}$ were characterised at micro-scale level using Scanning Electron Microscopy (SEM), Energy Dispersive X-ray (EDX – data in wt%) and X-ray Diffraction (XRD). The SEM (a Hitachi SM2400) was also used to collect EDX and Autopoint EDX data. XRD data was collected using a Siemens Diffraktometer 5000 with a locked detector tube between '2θ' angles of 10 to 90° ('θ' the X-Ray angle of incidence) and a Cu Kα source. To determine the phases present on the wear scar, the XRD data was interpreted using the associated DIFAC-DOS/DIFAC+ software and diffraction pattern database.

A simple temperature versus sliding speed wear map was constructed for the Nimonic 80A versus Incoloy 800HT combination using the weight change data and observations. Data collected by Rose [6] was used for the 0.654 $m.s^{-1}$ observations (tests not repeated at this speed), the current study concentrating on 0.314 and 0.905 $m.s^{-1}$. Due to Rose collecting the 0.654 $m.s^{1}$ data after 9,418 m (not 4,522 m), the wear map in this case only shows types of wear and does not include weight data. Counterface EDX analysis is reported at 750°C only, due to difficulties sectioning suitable samples and a need to reuse counterfaces for continued testing. Due to this need for reuse, Incoloy 800HT counterface wear was not quantitatively assessed in the current study.

Micro-hardness data for metallic transfer and 'glaze' layers was collected using a Buehler Micromet II tester (Vickers diamond pyramidal indenter, load 50g, dwell time 12s). To enable micro-hardness testing with a minimal error, high temperature samples were withdrawn from the test furnace as soon as each sliding test ended and air cooled to allow the sample sliding surface to be retained in as close to its "as slid" state as possible. Failure to do this may have led to partial annealing and softening of any work-hardened structures generated, especially at the highest test temperatures.

2.2 Characterisation of Evolved Layers at 750°C

Samples slid at 0.314 and 0.905 $m.s^{-1}$ (750°C) were cross-sectioned, after which the cross-sections underwent SEM study and profiled using a system called 'Autopoint'. In other words, EDX was done at regular intervals through a cross-section, starting at the worn surface and passing through the wear-affected layers into the undeformed substrate. Such analysis helped determine effects such as degree of transfer, mixing of sample and counterface material and preferential elemental diffusion. The information was used to predict a likely order of events during the sliding process.

3. Results

3.1 Weight Change and Friction Data

3.1.1 0.314 $m.s^{-1}$

a) Weight change data

At 0.314 $m.s^{-1}$, fairly small changes in Nimonic 80A sample weight were observed throughout the entire test temperature range (Fig. 2 – negative values indicate weight loss). The largest losses were

at 390°C (weight change -0.055(0) g) with continued moderately high losses up to 570°C. Bar another minimum at 630°C (weight change -0.042(2) g), weight loss decreased on approaching 750°C, at which temperature there was a slight gain (0.001(8) g).

b) Coefficient of friction data

An unsettled 'run-in' period was observed on commencing sliding at 0.314 $m.s^{-1}$, this quickly giving way to a more settled 'steady state' phase. There was no clear trend for 'run-in' data with rising temperature (Fig. 3a); 'run-in' values rose almost immediately from zero to a mean of ~1.12 at R.T., ~1.38 at 270°C and 510°C and ~1.13 at 750°C, with up to ~20% sample-to-sample variation.

However, there was a clear downward trend with temperature for 'steady state' data; coefficient of friction at 0.314 $m.s^{-1}$ decreased from 0.81-0.875 at R.T. to ~0.6 at 270 and 510°C, reaching a 0.42-0.5 minimum at 630°C, before rising back to 0.55-0.66 at 750°C. Sample-to-sample variation remained fairly low at 0.314 $m.s^{-1}$, being no more than 8 to 10% at all temperatures.

3.1.2 0.905 $m.s^{-1}$

a) Weight change data up to 4,522 m of sliding

At 0.905 $m.s^{-1}$ / 4,522 m, there were small Nimonic 80A sample weight gains at almost all test temperatures (Fig. 2), starting at 0.009(0) g at R.T. and rising to maximums of 0.019(6) g at 450°C and 0.019(9) g at 570°C. Above 570°C, weight gain decreased, with a small loss at 750°C (weight change -0.004(1) g). These results indicate material build-up on the Nimonic 80A surface.

b) Weight change data up to13,032 m of sliding

Continued sliding up to 13,032 m at 0.905 $m.s^{-1}$ up to 570°C resulted in reduced weight gain values compared to those after 4,522 m; in other words, some but not all of the material gained by the Nimonic 80A samples after 4,522 m was lost. Typical weight change values after 13,032 m were 0.005(8) g at R.T. (compared to 0.009(0) g after 4,522 m), most noticeably 0.000(7) g at 510°C (0.017(6) g after 4,522 m) and 0.011(2) g at 570°C (0.020(9)g after 4,522 m).

At 630°C and 690°C, the weight gains after 4,522 m (weight changes of 0.042(2) g and 0.005(3) g respectively), became weight losses after 13,032 m (-0.004(8) g and -0.001(9) g). At 750°C, a small weight loss after 4,522 m (-0.004(1) g) became a slight gain (0.001(8) g); this temperature did not follow normal trends.

c) Coefficient of friction data at 0.905 $m.s^{-1}$

An unsettled 'run-in' period followed by a more settled 'steady state' phase was observed at 0.905 $m.s^{-1}$ as it has at 0.314 $m.s^{-1}$. During unsettled 'run-in', there was no clear trend in coefficient of friction with rising temperature, values rising from zero to 1.08 at R.T., 1.22 at 270°C, 1.33 at 510°C and 1.04 at 750°C with sample-to-sample variation of ~20%.

There was a clear downward trend with increasing temperature during the 'steady state' phase, with values decreasing from 0.68-0.83 at R.T., to 0.65-0.74 at 270°C, 0.52-0.65 at 510°C, and (attributable to 'glaze' formation) 0.20-0.35 at 750°C. Variation apparently increased with temperature, being ≤10% at R.T. and 270°C, and ~25% at 510°C and 750°C; this may be due to lower recorded friction relative to a steady absolute variation (±0.1 to 0.15). Also, lower friction and higher variability at 0.905 $m.s^{-1}$ compared to 0.314 $m.s^{-1}$ may be due to speed-induced increased vibration reducing sample-counterface contact time; true friction at 0.905 $m.s^{-1}$ may be much higher.

At 0.905 $m.s^{-1}$, particularly large drops in friction (from >0.8 and at times 1 to between typically 0.3 and 0.5 – despite the vibration) occurred during sliding at 'glaze' forming temperatures (i.e. 630°C, 690°C and 750°C). Such observations have been attributed to the onset of mild oxidational wear and 'glaze' layer formation with associated elimination of metallic contact [2]. The mean distance to this transition decreased with temperature:
i.e.

- ~5,430 m (100 minutes) at 630°C (observed on continued sliding to 13,032 m);
- ~2,172 m (40 minutes) at 690°C and;
- ~869 m (16 minutes) at 750°C.

Such a pattern was not observed at 0.314 $m.s^{-1}$.

3.2 Optical and SEM Morphology – Nimonic 80A versus Incoloy 800HT

3.2.1 0.314 $m.s^{-1}$

Optical (Fig. 4) and SEM (Fig. 5) examinations indicated 'severe wear' (wear surfaces were bright, metallic and highly damaged) at 0.314 $m.s^{-1}$ with high levels of metal transfer at R.T. and 270°C leading to transfer layer formation on Nimonic 80A wear surfaces (Figs. 4 and 5). Both R.T. and 270°C debris (SEM – Fig. 6) were flat, metallic, irregularly shaped and platelet-like in nature, suggesting generation by a delamination mechanism [59]. These debris were generally between 20 µm and 1 mm across.

Metallic transfer at 0.314 $m.s^{-1}$ was much reduced between 390 and 570°C, with only a few patches of transferred material on the largely exposed Nimonic 80A wear scar (Fig. 4 – Fig. 5 also shows the 510°C wear surface under SEM). This decreased transfer coincided with increasing wear scar surface oxidation with temperature, visible as discolouration at 390°C and 510°C (Fig. 4 – this oxide did not form into compacted oxide layers). The SEM micrograph at 510°C also shows slight evidence of fine, parallel lines in the direction of sliding (previously unreported [1]), hinting at oxide abrasive action. Trace amounts of very fine oxide debris (< 1µm in size) were detected on the larger, flat platelet-like metallic debris at ≥390°C, quantities increasing with temperature.

Traces of 'glaze' at 0.314 $m.s^{-1}$ first appeared at 570°C with significant 'glaze' layer development at ≥630°C; 'glaze' development increased with temperature, coinciding with decreased wear (Fig. 1).

A transfer layer reappeared in such cases (≥630°C), overlaid by the 'glaze'. A substantial portion of debris was still flat, metallic, platelet-like and irregularly shape (indicative of generation by delamination [59] – debris size was still 20 µm to 1 mm across – Fig. 6), but this was accompanied by increasing oxide debris. This oxide debris remained of a very fine, at <1 µm and in some cases <300 nm in size, noticeable on the larger metallic debris surfaces at 750°C (Fig. 6).

3.2.2 0.905 $m.s^{-1}$

At 0.905 $m.s^{-1}$, a high metallic transfer 'severe wear' regime dominated between R.T. and 630°C, accompanied by transfer layer formation with comprehensive wear scar coverage regardless of sliding temperature (Figs. 4 and 7). Surface oxidation at ≥390°C (most visible as discolouration on the wear scar surfaces) did not apparently affect metallic transfer at 0.905 $m.s^{-1}$.

Metallic debris production up to 630°C, again flat, platelet-like and of size between 20 µm and 1 mm (removal by a delamination mechanism [59] – Fig. 8), was at 0.905 $m.s^{-1}$ not noticeably different to 0.314 $m.s^{-1}$. Trace amounts of oxide debris were present amongst the metallic debris at ≥390°C, accompanying increasing wear scar discoloration at higher temperatures. However, there was no hint of this oxide acting abrasively (as at 0.314 $m.s^{-1}$ and 510°C).

At ≥630°C, 'glaze' developed on top of the metallic transfer layer at 0.905 $m.s^{-1}$ (Fig. 4). At 630°C, patchy 'glaze' formed after 4,522 m of sliding with more substantial but still limited 'glaze' layer development after 13,032 m. At 690°C and especially 750°C (Figs. 4 and 7), comprehensive 'glaze' layer development was observed after only 4,522 m (persisting to 13,032 m). Oxide debris production increased also (Fig. 8), repeating the pattern of metallic debris with increased oxide debris on raising test temperature from 630°C to 750°C, seen at 0.314 $m.s^{-1}$. As these 'glaze' layers developed, the level of metallic transfer decreased slightly at 0.905 $m.s^{-1}$, particularly at 750°C.

3.3 EDX Analysis

3.3.1 0.314 $m.s^{-1}$

The 0.314 $m.s^{-1}$ EDX data indicated variation depending on whether or not a metallic transfer layer was present on the Nimonic 80A surface. At R.T., the surface layer composition closely matched that of the Incoloy 800HT counterface (~30% Ni, ~23% Cr, ~44% Fe), with only minimal changes at 270°C (~30% Ni, ~24% Cr, ~41% Fe). There was no significant mixing and debris composition also closely matched Incoloy 800HT.

Between 390°C and 570°C, only the limited metallic transfer areas gave compositions different from the mostly exposed, highly worn Nimonic 80A substrate indicating only a little mixing. At 510°C, more exposed areas gave intermediate but still high Ni compositions (averaging ~51% Ni, ~29% Cr, ~13% Fe), whilst transferred areas were generally closer to Incoloy 800HT (~29% Ni, ~25% Cr, ~40% Fe).

For samples worn at ≥570°C where 'glaze' formed overlying a limited metallic transfer layer, the 'glaze' gave values similar to Incoloy 800HT (23% Ni, 31% Cr, 42% Fe). Exposed areas of metallic transfer layer were of intermediate composition between Nimonic 80A and Incoloy 800HT (~32% Ni, 34% Cr, ~20% Fe). Thus some sample-counterface mixing is indicated during at least part of the earlier metallic transfer stage.

The composition of the accompanying metallic debris formed at ≥390°C was more variable depending on the debris particle or particles analyses, with some matching the Incoloy 800HT counterface (this the main source of material) and some more intermediate between that and the Nimonic 80A sample. Metallic debris composition was most variable (and most likely of intermediate levels – ~23% to ~51% Ni, ~14% to 41% Fe; Cr levels remained at around ~28%) at mid-range temperatures (390°C, 450°C and 510°C), where transfer layers on the sample were incomplete and some material removal from it was still possible; the same applied to the trace oxide debris produced at these temperatures. The increasing proportions of oxide debris present at ≥570°C (~25% Ni, ~30% Cr, ~40% Fe) closely matched Incoloy 800HT composition.

3.3.2 0.905 $m.s^{-1}$

At 0.905 $m.s^{-1}$ / 4,522 m with metal transfer to Nimonic 80A across the entire test temperature range, transfer layer composition closely matched Incoloy 800HT (Fe varying between ~37 and 41%, Ni rising slightly from 23 to 28%, Cr dropping slightly from 32 to 26%). The 'glaze' layers overlying the Incoloy 800HT sourced-transfer between 630°C and 750°C were of similar composition to them.

Sliding up to 13,032 m (at 0.905 $m.s^{-1}$) gave a more intermediate, mixed metallic transfer layer composition at all temperatures (on average 35% Ni, 29% Cr and 30% Fe, with typically 2 to 3% variation). The only exception was at 750°C, where 'glaze' and the transfer layer composition (both ~23% Ni, ~31% Cr, ~41% Fe) closely matched Incoloy 800HT.

The metallic debris at 0.905 $m.s^{-1}$ was also close to Incoloy 800HT in composition, although some debris particles contained higher Ni (up to ~35%), indicating a Nimonic 80A contribution; this was also true of the trace oxide debris observed between 390 and 570°C. At ≥630°C, loose oxide debris composition more consistently matched that of the Incoloy 800HT counterface.

3.3.3 Cross-sectional Analysis and Autopoint EDX

Cross-sectional Autopoint EDX analysis of Nimonic 80A (0.314 $m.s^{-1}$ / 4,522 m and 0.905 $m.s^{-1}$ / 13,032 m – Figs. 9 and 10 respectively, both 750°C), indicated an Incoloy 800HT-consistent composition within the ~1 µm thick 'glaze' layer (Ni ~24%, Cr ~27%, Fe ~40% at 0.314 $m.s^{-1}$; Ni ~22%, Cr ~27%, Fe ~38% at 0.905 $m.s^{-1}$). The main source of 'glaze' material was transfer from the Incoloy 800HT counterface, with little sliding speed-induced variation.

At 0.314 m.s^{-1}, the 'glaze' overlay a mixed metallic and oxide layer extending to between 32 µm and 37 µm depth (34 µm in Fig. 9) of intermediate compositions between Nimonic 80A and Incoloy 800HT; below this there was only Nimonic 80A substrate. Mixing within this layer was incomplete, some areas closely matching Nimonic 80A composition and others of intermediate composition (Ni varied between 25 and 70%, Cr between 10 and 55% and Fe between 5 and 22%). Notable in Fig. 9 is an area of material of similar composition to Nimonic 80A (~69% Ni, ~12% Cr and ~10% Fe) at 4 µm depth and also an area of intermediate composition near the layer's base at ~30 µm depth (~28% Ni, ~52% Cr and ~5% Fe). There is no clear explanation for the high Cr at ~30 µm, though diffusion from the Ni-rich region (where Cr is at ~12%) is possible.

At 0.905 m.s^{-1}, the 'glaze' overlay an oxide-only layer existing to between 10 and 14 µm depth (14µm in Fig. 10) and then a mixed metal / oxide layer from 14 µm to between 40 and 45 µm depth (41 µm in Fig. 10); both were of composition close to Incoloy 800HT. Variations within the mixed metal-oxide layer were originally attributed to limited mixing with Nimonic 80A [1] (between 22 - 31% Ni, 20 - 43% Cr and 24 - 41% Fe). However, Cr peaks match those of O in this region, which also coincide with troughs in Fe and Ni; this suggests a limited diffusion and preferential oxidation effect. A greater Nimonic 80A contribution (with higher Ni) started below ~33 µm depth, with 40 to 45 µm (this varied between samples) marking the beginning of the Nimonic 80A substrate.

The higher than expected Al in Nimonic 80A (Table 1) showed slight evidence of diffusion to the Nimonic 80A substrate / transfer layer interface at 0.314 m.s^{-1} (Fig. 9) but not 0.905 m.s^{-1} (Fig. 10).

EDX Mapping of 750°C samples slid at both sliding speeds (not shown [1]) roughly verified the Autopoint EDX analysis, with generally high Fe and low Ni in the surface layers, variance in Cr and a bias of O towards the uppermost debris layers (with some variance and unoxidised areas of metallic transfer within the layers) and 'glaze'. There was occasional trace O along the transfer layer / Nimonic 80A substrate interface, especially at 750°C / 0.905 m.s^{-1}, indicating limited oxidation prior to early metallic transfer. Additionally, some limited Al concentration was confirmed at the transfer layer / Nimonic 80A interface at 0.314 m.s^{-1}, but not at 0.905 m.s^{-1}.

Distinguishing between 'glaze' and underlying debris was difficult at times, as is clear from the Autopoint cross-sections (Figs. 9 and 10). However, the absence of coarser debris within the top ~2 µm of debris surface enabled a rough differentiation of 'glaze'.

3.4 XRD Analysis

Metallic 'face-centred cubic' $Ni_{2.9}Cr_{0.7}Fe_{0.36}$ phase was present in all samples regardless of sliding speed or temperature. This phase was detected for both metallic Nimonic 80A and Incoloy 800HT.

No oxide phase was detected between R.T. and 510°C at either 0.314 m.s^{-1} or 0.905 m.s^{-1}, despite increasing oxide discoloration of wear scar surfaces and slight evidence of oxide debris at ≥390°C.

$NiCr_2O_4$ oxide nichromate phase was detected only at 'glaze' forming temperatures (≥570°C at 0.314 $m.s^{-1}$; ≥630°C at 0.905 $m.s^{-1}$).

XRD alone could not determine if source material for the metallic transfer layers or 'glaze' (at high temperature) was Nimonic 80A or Incoloy 800HT, as phases generated were of high Ni and Cr content ($Ni_{2.9}Cr_{0.7}Fe_{0.36}$ and $NiCr_2O_4$). Only by using EDX (Section 3.3) to supplement XRD was it possible to determine Incoloy 800HT as the dominant source of metallic transfer plus the 'glaze' layers formed at ≥570°C (≥630°C at 0.905 $m.s^{-1}$). Also, EDX data suggests with Fe at 40% for both 0.314 and 0.905 $m.s^{-1}$ / 4,522 m, this should appear within the 'glaze' oxide phase (possibly as $NiCrFeO_4$) and why this is not so is uncertain.

3.5 Micro-hardness Testing – Nimonic 80A versus Incoloy 800HT

The mean hardness of transfer layers formed at R.T. (Table 2) were little different to that for the unworn Nimonic 80A substrate (5.23 GPa). However, as the transfer layer on the Nimonic 80A was predominantly Incoloy 800HT-sourced (EDX data – Section 3.3), if the hardness data is compared to that of Incoloy 800HT (2.15 GPa) then the transferred material shows a high degree of hardening.

No data was collectable for 0.314 $m.s^{-1}$ samples between 390°C and 570°C, due to the absence of transfer layers on the Nimonic 80A (patchy, isolated transfer at best). However, where comprehensive, largely Incoloy 800HT-sourced transfer layers continued to form on the 0.905 $m.s^{-1}$ / 4,522 m Nimonic 80A samples over the same temperature range, data indicated continued hardening despite the elevated sliding temperatures (Table 2).

The hardness of surface 'glaze' layers formed at 750°C was extremely high (~20.0 GPa at 0.314 $m.s^{-1}$ and ~18.1 GPa at 0.905 $m.s^{-1}$ / 4,522 m) and well in excess of the unworn Nimonic 80A substrate (Table 2). No collapse of the 'glaze' layers was noted and indenter penetration into the 'glaze' did not reveal an underlying powder layer (seen with both Nimonic 80A and Incoloy MA956 when slid at high temperature against Stellite 6 [1,4,7,23]).

Cross-sectional profiling of Nimonic 80A indicated a little evidence of hardening of near-surface material at both 0.314 and 0.905 $m.s^{-1}$, with hardness as high as 7 or 8 GPa in or near to the region of the transfer layer (Fig. 11). No clear trend with temperature was evident, except greater general hardness of Nimonic 80A slid at 750°C; it is possible such higher hardness values on cooling are due to precipitation hardening effects whilst holding Nimonic 80A at 750°C [60].

3.6 Incoloy 800HT Counterface Wear Scar Morphology and Analysis

A grooved, worn surface formed on the Incoloy 800HT counterface at all temperatures between R.T. and 750°C, regardless of sliding speed (Fig. 12 shows the wear scars created at 0.314 $m.s^{-1}$; those at 0.905 $m.s^{-1}$ were near-identical). Between R.T. and 450°C, the counterface underwent high wear with limited transfer layer development indicating transfer and back-transfer of metallic material to

and from the Nimonic 80A sample. Discoloration of wear scar surfaces due to limited oxidation at 390 and 450°C coincided with reduced transfer layer development.

At 510°C and above, discrete asperities of metallic material appeared in the counterface wear track (the depth of which was up to 1.5 mm into the counterface surface), their quantity increasing with temperature. Asperity height was sometimes up to ~1.5 mm above the original counterface surface between 630°C and 750°C, with a slightly lower asperity concentration at 0.905 $m.s^{-1}$.

'Glaze' formed on the counterface asperity peaks at ≥570°C (0.314 $m.s^{-1}$) or ≥630°C (0.905 $m.s^{-1}$), matching 'glaze' forming temperatures on the Nimonic 80A. This 'glaze' formation was accompanied by large quantities of easily dislodged loose oxide debris appearing within the Incoloy 800HT counterface wear track. Asperity 'glaze' layer composition was similar to the 'glaze' layers on the Nimonic 80A, that is to say not too dissimilar to the Incoloy 800HT, regardless of sliding speed (~29% Ni, 23% Cr and 45% Fe after sliding at 0.314 $m.s^{-1}$ / 4,522 m; ~24% Ni, ~30% Cr and ~41% Fe for 0.905 $m.s^{-1}$ / 4,522 m with 0.905 $m.s^{-1}$ / 13,032 m near-identical).

4. Wear Map for Incoloy MA956 versus Incoloy 800HT

It is possible to construct a wear map for Nimonic 80A (sample) worn against Incoloy 800HT (counterface) using the 0.314 and 0.905 $m.s^{-1}$ information presented and also previous 0.654 $m.s^{-1}$ data [6] (Fig. 13). This describes sample wear behaviour as a function of sliding speed and temperature showing three main regions of wear behaviour. Reference is made to previously suggested wear mode descriptions [24, 25] based on Quinn's 'mild' and 'severe' wear [61]

No weight loss data is presented on the wear map, due to the collection of Rose's 0.654 $m.s^{-1}$ data after 9,418 m [6] and not 4,522 m as for 0.314 and 0.905 $m.s^{-1}$ in the current study. Regions over which XRD observations were made are also displayed.

At 0.314 $m.s^{-1}$:

1. A '*standard severe wear*' regime dominates at R.T. and 270°C with high levels of metallic transfer from the Incoloy 800HT and adhesion to the Nimonic 80A. A work-hardened transfer layer forms on the Nimonic 80A wear surface, reducing Nimonic 80A wear.

2. At 390°C and 450°C, metallic '*standard severe wear*' continues. However, transfer is much reduced due to surface oxidation inhibiting adhesion and transfer layer formation. Consequently, Nimonic 80A wear increases.

3. The 'severe wear' at 510°C is similar to that at 390°C and 450°C, however, assisted by some oxide abrasion (i.e. '*abrasion-assisted severe wear*').

4. Between 570°C and 750°C, limited metallic transfer from the Incoloy 800HT counterface to the Nimonic 80A is accompanied by oxidation, forming an intermediate composition mixed metal-oxide transfer layer. This is later overlaid by an Incoloy 800HT-sourced nichromate-phase 'glaze' layer as '*protective mild wear*' is established.

The following behaviour was observed at 0.654 $m.s^{-1}$ by Rose [6] and also in the current study at 0.905 $m.s^{-1}$:

1. A '*standard severe wear regime*' dominates between R.T. and 570°C, with high levels of metallic transfer from the Incoloy 800HT and adhesion to the Nimonic 80A to form a work-hardened transfer layer. This layer reduces Nimonic 80A wear.

2. High levels of initial metallic transfer from the Incoloy 800HT counterface to the Nimonic 80A along with some oxidation, produce a predominantly Incoloy 800HT-based mixed metal-oxide layer transfer layer between 630°C and 750°C.

   Increasing sliding speed to 0.905 leads to greater transfer than at 0.654 $m.s^{-1}$ [1] (0.654 $m.s^{-1}$ samples [6] were examined – not discussed here). Also, 'glaze' formation and establishment of '*protective mild wear*' are delayed at 0.905 $m.s^{-1}$; there is less 'glaze' development at 0.905 $m.s^{-1}$ after 13,032 m of sliding than at 0.654 $m.s^{-1}$ after 9,418 m [6].

There was no evidence of a purely '*abrasive mild wear*' regime (oxide prevents metallic contact but remains loose, acting abrasively to encourage high wear) [23,24], nor of So's '*extrusive wear*' regime [62] observed under extreme conditions of temperature, load and sliding speed.

5. Discussion

5.1 Sliding Speed

5.1.1 0.314 $m.s^{-1}$

Between R.T. and 750°C, four different regimes depending upon temperature are possible when Nimonic 80A is worn against an Incoloy 800HT counterface.

A 'standard severe wear' mode dominates at R.T. and 270°C with enhanced metallic transfer forming an Incoloy 800HT-sourced, work-hardened metallic layer on the Nimonic 80A (Figs. 4 and 5 / Table 2a), which protects the Nimonic 80A surface and prevents excessive material removal from it. An absence of oxide debris allows ready metallic adhesion and consequent development of the transfer layers. Flattened metallic debris (Fig. 6) is formed by a delamination mechanism [59], either by direct removal from the highly worn Incoloy 800HT counterface or by limited removal from the Incoloy 800HT-sourced transfer layer on the Nimonic 80A.

This 'standard severe wear' mode also dominates between 390°C and 510°C (Figs. 4 and 5), however, there is increased Nimonic 80A wear caused by:

1) the absence of a protective transfer layer (Figs. 4 and 5); and

2) greater softening of metallic surfaces with increased temperature (Table 3) [6].

Material removal is once again by a delamination mechanism [59], evidence by the large, flattened nature of generated debris (Fig. 6) regardless of debris source (Nimonic 80A or Incoloy 800HT).

A metallic transfer layer does not form due to increasing oxidation of the exposed Nimonic 80A surface with temperature (visible as discolouration on the wear surface – Fig. 4 shows this at 510°C), inhibiting Incoloy 800HT counterface-sourced metallic debris adhesion to the Nimonic 80A wear surface. Additionally, oxidation rate is insufficient to overcome the low retention and residency times, and high debris ejection levels at the wear interface. Consequently the oxide is also unable to develop into significant debris layers and afford any protection to the Nimonic 80A; this limited oxide development and retention in fact increases wear (some debris is now Nimonic 80A-sourced).

Whilst severe wear is dominant between 390°C and 510°C, a slight oxide abrasive element at 510°C (slight evidence of parallel groves in the direction of sliding – Fig. 5b) slightly further assists wear. This suggests a modification in wear mechanism to a regime referred to elsewhere as 'abrasion assisted severe wear' [24, 25].

The effect of debris retention on wear is demonstrated by testing without Nimonic 80A sample reciprocation at 510°C with a 0.314 $m.s^{-1}$ rotating counterface sliding speed [1]. Increased retention allows patchy nichromate 'glaze' development indicating significant oxidation and also that enhanced removal with sample reciprocation prevents 'glaze' development from such oxide.

Finally between 570°C and 750°C, fine Ni-Cr-Fe oxidational debris is produced by enhanced oxidation of contacting Nimonic 80A and Incoloy 800HT surfaces; the primary source remains Incoloy 800HT (Section 3.3.1). Oxide debris development now exceeds losses by ejection and the debris can thus build up and sinter on the wear surfaces forming high hardness (~19.97 GPa at 750°C – Table 2), wear resistant nichromate-phase 'glaze' layers (Figs. 4 and 5). Such oxide layer formation becomes more rapid with rising temperature, reducing severe wear during early sliding (as evidenced by decreased wear scar size – Fig. 4) and promoting the more rapid onset of 'protective mild wear'. The development of these 'glaze' layers also prevents any loose oxide acting abrasively against the underlying metal.

The brief period of early severe wear with metallic transfer layer development (and back-transfer forming counterface asperities as oxide increases – see Section 5.3) is still sufficient to cause significant damage, because of rapid material removal due to reduced Nimonic 80A and especially Incoloy 800HT hardness at 'glaze' forming temperatures. This period ends as increasing debris oxidation inhibits adhesion prior to the onset of 'protective mild wear'.

5.1.2 0.905 $m.s^{-1}$

Two wear regimes are possible for the Nimonic 80A / Incoloy 800HT (counterface) system at 0.905 $m.s^{-1}$, depending on temperature.

Firstly at R.T. and 270°C, a high friction 'standard severe wear' regime dominates mirroring that at 0.314 $m.s^{-1}$, with flattened metallic debris generation by a delamination mechanism [59] (Fig. 8); much of the material removed from the Incoloy 800HT adheres to the Nimonic 80A surface to form a work-hardened metallic transfer layer (Figs. 4 and 7 / Table 2). This protects the Nimonic 80A surface from enhanced wear, as shown by the low losses on continued sliding to 13,032 m (Fig. 2).

Transfer of metallic Incoloy 800HT material to Nimonic 80A continues at 0.905 $m.s^{-1}$ between 390°C and 570°C (Figs. 4 and 7), with reduced interference to metallic adhesion by oxide compared to 0.314 $m.s^{-1}$ (though still enough to cause discoloration). At 0.905 $m.s^{-1}$, debris removal rates are higher and residency lower; also, any oxide forming on wear surfaces have insufficient development time between surface contacts and removal, to reach adhesion-inhibiting levels. Metallic debris thus continues to adhere and form transfer layers up to 570°C. There is also no hint of oxide abrasive action (as seen at 0.314 $m.s^{-1}$ and 510°C) probably due to this lower residency.

Metallic transfer levels at 0.905 $m.s^{-1}$ are higher than at 0.314 $m.s^{-1}$, also because of greater Incoloy 800HT removal from the heavily worn counterface. This transfer was so high during early wear that sample weight clearly increased during the first 4,522 m of sliding at 0.905 $m.s^{-1}$ (Fig. 2). Additionally, increased Incoloy 800HT counterface wear, material removal and transfer to Nimonic 80A on raising temperature from R.T. to 570°C (Fig. 9a) is probably due to thermal softening of Incoloy 800HT (Table 3).

The slight reductions in Nimonic 80A sample weight on continued sliding beyond 4,522 m (up to 13,032 m – Fig. 2) are due to an absence of large-scale transfer coupled with limited metallic material loss through wear. The work-hardened metallic transfer layer formed during early sliding (pre-4,522 m), now protects Nimonic 80A from further enhanced wear. Some transfer and redeposition to and from both sample and counterface continues on sliding up to 13,032 m, leading to mechanical mixing or alloying [37] within the transfer layer on the Nimonic 80A (Section 3.3.2). Mixing remains incomplete, however, and a heterogeneous layer with variable levels of Ni, Cr and Fe results.

At 0.905 $m.s^{-1}$ / ≥630°C, early 'severe wear' with transfer layer formation gives way to 'protective mild wear' as 'glaze' layer development inhibits metallic adhesion; this replicates the situation at 0.314 $m.s^{-1}$ / ≥570°C. The rate of 'glaze' layer development increases with temperature, as indicated by limited 'glaze' formation after 13,032 m at 630°C (with only patchy 'glaze' after 4,522 m), compared to more comprehensive 'glaze' layers after 4,522 m at 690°C and especially 750°C. This increasingly rapid 'glaze' formation also reduces the average severe-to-mild-wear transition

distance for friction values, from ~5,430 m at 630°C, to ~2,172 m at 690°C and ~869 m at 750°C. These high hardness (18.06 GPa at 750°C – Table 2), nichromate-phase 'glaze' layers (Figs. 4 and 7) form rapidly enough at 750°C to arrest overall wear (Fig.1).

5.2 Oxide Composition and Effect on 'Glaze' Formation

The $NiCr_2O_4$ nichromate oxide indicated by EDX and XRD readily sinter to form the observed 'glaze' layers when sliding Nimonic 80A against Incoloy 800HT at ≥ 570°C (0.314 $m.s^{-1}$) / ≥ 630°C (0.905 $m.s^{-1}$). It is suggested this greater sinterability is due to the 'glaze'-forming oxide's close compositional match to its Incoloy 800HT source, which contains 40% Fe. This is in contrast to the abrasive, poorer 'glaze'-forming NiO / Cr_2O_3 individual oxides generated at high sliding speeds and similar temperatures for Nimonic 80A versus Stellite 6 [1,4,7,24]; NiO and Cr_2O_3 appear to require high debris retention (i.e. 'pin-on-disc' [16,18-22]) to encourage sintering and 'glaze' formation.

Moreover, the high Fe level suggests an Fe-containing $NiCrFeO_4$ phase is more likely and an Fe-containing oxide phase ($Cr_{1.3}Fe_{0.7}O_3$) has previously been shown to readily form 'glaze' at higher sliding speed [1,23,25] at ≥630°C. However, Co-containing oxides generated with Stellite 6 as at least one member of the wear pair still exhibit greater 'glaze' forming tendencies [1, 4-7, 23,24].

5.3 Counterface

Between R.T. and 510°C, the Incoloy 800HT counterface wear scar forms a grooved profile, in which a transfer layer develops due to removal and readhesion of metallic material irrespective of temperature and sliding speed. Even at 0.314 $m.s^{-1}$ where a comprehensive transfer layer does not form on the Nimonic 80A at ≥390°C, counterface transfer layer formation persists due to continued readhesion. Reduced Incoloy 800HT counterface oxidation under sliding conditions may mean debris readhesion is less inhibited than on Nimonic 80A.

There is greater damage to the Incoloy 800HT counterface wear track at 'glaze'-forming temperatures (570°C at 0.314 $m.s^{-1}$ / 630°C at 0.905 $m.s^{-1}$ up to 750°C) and a trough of ~1.5 mm depth forms at both 0.314 and 0.905 $m.s^{-1}$, due to material removal and transfer to the Nimonic 80A. Some metallic material readheres to the Incoloy 800HT inside the wear scar to form asperities, some rising to ~1.5 mm above the original unworn surface; these asperities can only have been created by back-transfer (Fig. 12). As the only areas to come into contact with the sample transfer layers are the asperities, it is the peaks of these to which later 'glaze' formation is restricted.

At 750°C, the 'glaze' composition on the transfer layers overlying the Nimonic 80A matched that of the Incoloy 800HT. As the transfer layers underlying the 'glaze' on the sample are mixed composition, the only possible source of such composition oxide is the Incoloy 800HT. The 'glaze' layers on the counterface asperities are also of composition matching Incoloy 800HT, thus so must be the back-transferred metallic asperities.

The asperities must form later in the sliding process when Incoloy 800HT can no longer transfer to the Nimonic 80A sample (i.e. when increasing oxidation in the transfer layer inhibits further metallic debris adhesion), thus favouring back-transfer. 'Glaze' formation must only begin after back-transfer has created the counterface asperities and they have begun to interact with the highly oxidised layer on the Nimonic 80A transfer layer surface. Additionally, some oxidized debris is either ejected or collected as loose material in the base of the counterface wear track.

Sliding speed has no obvious effect on counterface wear scar morphology, though asperity formation at 0.905 $m.s^{-1}$ and 'glaze' forming temperatures may be slightly less.

5.4 Multi-Layer Development at 750°C

The formation of the multi-layer debris structures on Nimonic 80A slid against Incoloy 800HT (counterface) at 750°C and sliding speeds of 0.314 and 0.905 $m.s^{-1}$ (Figs. 9 and 10), follows a series of stages leading finally to generation of fine 'glaze' forming oxide (Fig. 10). The process suggested is similar to that for the Incoloy MA956 / Incoloy 800HT (counterface) wear pair [25], though with a stronger emphasis on Incoloy 800HT counterface wear and transfer from it.

1) Metallic debris is removed (leaving a trough ~1.5 mm deep on the counterface) and deposited onto the Nimonic 80A sample during early wear, generating a deformed, limited metallic debris layer overlying little damaged Nimonic 80A base metal. Early oxidation may be entrapped at the Nimonic 80A / redeposited metal interface.
2) Continued sliding later leads to progressive debris break-down and oxidation, this debris being deposited to form a mixed metal-oxide layer. Debris oxide levels increase with further sliding.
3) The continued increase in oxide levels results in an entirely oxidised sub-layer overlying the mixed metal-oxide debris layer, only at 0.905 $m.s^{-1}$.
4) This increasing oxidation inhibits further Nimonic 80A-bound transfer and adherence of Incoloy 800HT-sourced debris, which readheres inside the Incoloy 800HT counterface wear scar trough. This debris readhesion forms the aforementioned asperities, some ~1.5 mm in height above the original unworn counterface surface.
5) Incoloy 800HT-sourced nichromate phase fine oxide debris is generated by on-going debris break-down, from continued sliding contact between the mixed metal-oxide layer (at 0.314 $m.s^{-1}$) or completely oxidised sub-layer (at 0.905 $m.s^{-1}$), and the Incoloy 800HT counterface asperities.
6) This fine oxide debris is compacted and sintered into hard, wear protective 'glaze' layers, which develop on top of previously developed layers on the Nimonic 80A surface and also on the Incoloy 800HT counterface asperities. This stage represents the onset of 'protective mild wear'. Thereafter, as sliding continues, the 'glaze' is subject to continual break-down and reformation.

Sliding speed has a clear influence on the wear process. At 0.314 $m.s^{-1}$, material transferred from the Incoloy 800HT counterface initially mixes with Nimonic 80A sample-sourced material, however,

such mixing is incomplete resulting in an intermediate, heterogeneous composition in the mixed metal-oxide layer. At 0.905 $m.s^{-1}$, Incoloy 800HT counterface transfer dominates almost from the start of sliding and the layers formed are generally close to Incoloy 800HT composition.

The limited evidence of diffusion within the wear layers overlying the Nimonic 80A (Section 3.3.3) is attributable to a number of factors. Firstly, wear is generally dominated by Incoloy 800HT transfer to Nimonic 80A (despite initial mixing at 0.314 $m.s^{-1}$), effectively creating a 'like-on-like' sliding regime once the layers are established and 'glaze' forms. Secondly, a more homogeneous distribution of elements is ensured by a high degree of mixing at the sliding surface (post-layer formation), even if there is a Nimonic 80A contribution to the 'glaze'. Next, no species are readily available such as Al that could diffuse rapidly enough to overcome this mixing [1,23,25].

There is sufficient time for the limited diffusion effects observed within the mixed metal-oxide layer as the Incoloy 800HT-dominated material beneath the 'glaze' surface is only directly involved early in the wear process during this layer's formation. It's overlaying by the 'glaze' layers (and also the intermediate oxidised sub-layer at 0.905 $m.s^{-1}$) protects it from further wear-induced mixing.

Diffusion effects are only significant where there is a fast diffusing species such as Al (Incoloy MA956 versus either Stellite 6 [1,23] or Incoloy 800HT [1,25]) or where debris retention allows sufficient time for diffusion to occur. Examples of diffusion-induced non-uniform elemental distribution due to enhanced debris retention were observed by Wood et al. [63,64] during 'glaze' formation in a 'like-on-like' 'rotating collar' versus 'fixed disc' configuration at 600°C. There was sufficient diffusion to result in a layering of different oxides even at an elevated 3 $m.s^{-1}$ sliding speed, with both Tribaloy 400C [63] and Stellite 6 [64] sliding systems. This contrasted with more homogeneous oxide layer formation suggested by earlier literature [8].

Whilst there is some evidence of work-hardening effects within the Nimonic 80A immediately below the transfer layers (Fig. 11), it is unclear how much support this provides for overlying transfer layers and at high temperature, 'glaze' layers. During the current study, 'glaze' layers formed on top of previously generated transfer layers after early severe wear. It is these transfer layers that provide direct support to the 'glaze' layers and the effect of any work-hardening within the Nimonic 80A is limited at best. However, high wear observed prior to 'glaze' formation during elevated temperature sliding of Incoloy MA956 versus Incoloy 800HT, shows that lack of base metal mechanical support does not necessarily prevent 'glaze' formation [25].

5.5 Microstructure and Second Phases

Whilst the Nimonic 80A suffers some sliding damage, this is reduced as described by largely Incoloy 800HT metallic transfer layer protection and at high temperature by 'glaze' layer development. Even at higher temperatures, the Nimonic 80A samples retain their shape and do not suffer the deformation and creep seen on sliding Incoloy MA956 against Incoloy 800HT [25]. With a 'face-

centred cubic' structure across the entire temperature range, the 12 slip systems available would logically allow for extensive deformation and material removal. However, damage and material removal was primarily and preferentially observed on the similarly 'face-centred cubic' Incoloy 800HT counterface.

The greater resistance to deformation and material removal of Nimonic 80A compared to Incoloy 800HT, seems attributable to Nimonic 80A's enhanced mechanical properties and hardness at intermediate to high temperatures [6]. During the current study, there was little evidence Nimonic 80A underwent extensive softening and plastic deformation when slid against Incoloy 800HT.

These differing properties may in turn be influenced by relative levels of second phase in Nimonic 80A and Incoloy 800HT. Both materials still undergo continued deformation and ready material removal (at least during 'severe wear') and the low density of second phases (present to promote improved bulk mechanical properties) have not improved either alloy's wear resistance to a useful level [25]. This low second phase density may not be impeding dislocation movement and slip plane operation sufficiently to resist the high, localized shear stresses near the sliding surface [25] and may even assist delamination wear due to dislocation pile-up and coalescence to form sub-surface voids [59]. Whilst uncertain of the relative quantities of second phase in either alloy, levels of second phase within Nimonic 80A may be sufficient to better resist dislocation and slip plane operation during wear; wear properties and resistance to damage thus may be enhanced. How much alloy properties or second phase development were affected by the measured deviation from expected Nimonic 80A composition (Table 1) is unclear, despite maintenance of a 'face-centred cubic' structure. For instance, the extra Si (present to 2.33% rather than 0.1% – Table 1) may combine with other alloying elements to produce further wear modifying hard phases; the Si-based Laves phase in Tribaloy 400C is an example [63].

A comparative study – with varying levels of second phases and also without them – has previously been suggested to investigate their actual effect [25], using a 'like-on-like' combination of comparably heat treated alloys to minimize the effects of other variables.

If the current 'Nimonic 80A versus Incoloy 800HT' and previous 'Incoloy MA 956 versus Incoloy 800HT' [25] studies are compared with other data [1,4-7,23,24,49,50,65], low wear of alloys with a high scope for slip plane operation is only achievable with surface or bulk modification, or where sliding conditions favour extremely rapid protective layer formation (i.e. 'glaze' layer formation at extremely high temperature [47, 66]). Technically, alloys where 'glaze' forming oxides are readily generated and / or where the scope for slip plane operation and plastic deformation is restricted (i.e. 'hexagonal-close-packed' alloys – many of these Co-based [1,4-7,23,24,49,50,64,65]) still offer greater scope for more easily achievable reduced high temperature wear.

6. Conclusions

From the data collected it is possible to draw the following conclusions about the wear behaviour of Nimonic 80A (sample) slid against Incoloy 800HT wear pair slid at sliding speeds of 0.314 and 0.905 $m.s^{-1}$ (reciprocating 'block-on-cylinder' arrangement, 7N sample load), and temperatures of R.T. to 750°C.

1. A 'standard severe wear' regime at R.T. and 270°C results in formation of a wear-reducing, largely Incoloy 800HT-sourced work hardened transfer layer on the Nimonic 80A surface, regardless of sliding speed.
2. At 0.314 $m.s^{-1}$, 'standard' metallic severe wear continues up to 510°C, but surface oxidation inhibits metallic transfer. With no work-hardened transfer layer, Nimonic 80A wear increases. At 510°C, the reduced transfer metallic severe wear is also accompanied by a hint of oxide abrasion (i.e. 'abrasion assisted severe wear').
3. However, at 0.905 $m.s^{-1}$ an Incoloy 800HT-sourced work-hardened transfer layer continues to form on the Nimonic 80A surface up to 570°C; it is suggested this is due to a combination of greater Incoloy 800HT removal and transfer, and also enhanced removal / reduced residency of oxide at higher sliding speed.
4. A more mixed metal-oxide transfer layer forms on the Nimonic 80A at ≥570°C (0.314 $m.s^{-1}$), later overlaid by a protective 'glaze' layer. Raising sliding speed from 0.314 to 0.905 $m.s^{-1}$ delays this behaviour until 630°C.
5. Cross-sectional EDX profiling of 750°C Nimonic 80A samples indicates the formation of a multi-layered debris structure at both 0.314 and 0.905 $m.s^{-1}$ (Section 5.4), suggesting increasing oxidation as the debris is deposited before the overlying 'glaze' layer develops.
6. 'Glaze' formation reduces wear for the Nimonic 80A (sample) / Incoloy 800HT wear pair at high temperature (i.e. 'protective mild wear'), though not to acceptable levels due to continued early severe wear.
7. There is nothing to suggest either that the Nimonic 80A or Incoloy 800HT second phases, meant to improve bulk mechanical properties, improve wear resistance to a useful level. However, it cannot be discounted that Nimonic 80A's retention of shape and the preferential wear of the Incoloy 800HT may be due to differing levels of second phase.

Acknowledgements

Grateful acknowledgements are made to the UK Engineering Physics Science Research Council (EPSRC) and British Gas for their financial backing, Northumbria University for their day-to-day support and P.D. Wood, S.R. Rose and H.L. Du for their past contributions on this project.

References

[1] I.A. Inman, Ph.D. Thesis "Compacted Oxide Layer Formation under Conditions of Limited Debris Retention at the Wear Interface during High Temperature Sliding Wear of Superalloys", Northumbria University, UK (2003), published by 'Dissertation.com' (2006).

[2] I.A. Inman, S. Datta, H.L. Du, J.S. Burnell-Gray, S. Pierzgalski, Q. Luo "Microscopy of 'glazed' layers formed during high temperature sliding wear at 750°C", Wear 254 (2003) 461-467.

[3] S. Datta, I. Inman, H.L. Du, Q. Luo "Microscopy of 'glazed' layers formed during high temperature wear, Invited Talk at the Institute of Materials", Tribology Meeting, London, November 2001.

[4] I.A. Inman, S. Datta, H.L. Du, J.S. Burnell-Gray, S. Pierzgalski and Q. Luo "Studies of High Temperature Sliding Wear of Metallic Dissimilar Interfaces", Tribology International 38 (2005) 812–823.

[5] P.D. Wood, Ph.D. Thesis "The Effect of the Counterface on the Wear Resistance of Certain Alloys at Room Temperature and 750°C", Northumbria University, UK (1997).

[6] S.R. Rose, Ph.D. Thesis "Studies of the High Temperature Tribological Behaviour of Some Superalloys", Northumbria University, UK (2000).

[7] I.A. Inman, S.R. Rose, P.K. Datta "Development of a Simple 'Temperature versus Sliding Speed' Wear Map for the Sliding Wear Behaviour of Dissimilar Metallic Interfaces", Wear 260 (2006) 919–932.

[8] F.H. Stott, D.S. Lin, G.C. Wood "The structure and mechanism of formation of the "glaze" oxide layers produced on Ni-based alloys during wear at high temperatures", Corrosion Science 13 (1973) 449 - 469.

[9] M. Johnson, P. Moorhouse, J.R. Nicholls, DTI Industry Valve Project, 61-68 (1990).

[10] J-N. Aoh, J-C. Chen "On the wear characteristics of Co-based hardfacing layer after thermal fatigue and oxidation", Wear 250-251 (2001) 611.

[11] Singh, J. and Alpas, A.T. "High-temperature Wear and Deformation Processes in Metal Matrix Composites," Metallurgical and Materials Transactions A, 27 (1996) 3135-3148.

[12] F.H. Stott, J. Glascott, G.C. Wood "Factors affecting the progressive development of wear-protective oxides on Fe-base alloys during sliding at elevated temperatures", Wear 97 (1984) 93-106.

[13] M.G. Gee, N.M. Jennett "High resolution characterisation of tribochemical films on alumina", Wear 193 (1995) 133-145.

[14] P.D. Wood, P.K. Datta, J.S. Burnell-Gray, N. Wood "Investigation into the high temperature wear properties of alloys contacting against different counterfaces, Materials Science Forum", 251-254 (1997) 467-474.

[15] Wisbey, C.M. Ward-Close, Materials Science and Technology "Wear resistant surfaces on high temperature titanium alloy and titanium aluminide by diffusion bonding", 13 (1997) 349-355.

[16] J. Jiang, F.H. Stott, M.M. Stack, ”The effect of partial pressure of O on the tribological behaviour of a Ni-based alloy, N80A, at elevated temperatures”, Wear 203-204 (1997) 615-625.

[17] X.Y. Li, K.N. Tandon “Microstructural characterization of mechanically mixed layer and wear debris in sliding wear of an Al alloy and an Al based composite”, Wear 245 (2000) 148-161.

[18] J. Jiang, F. H. Stott, M. M. Stack “A generic model for dry sliding wear of metals at elevated temperatures” Wear 256 (2004) 973-985.

[19] J. Jiang, F. H. Stott, M. M. Stack “The role of triboparticulates in dry sliding wear” Trib. Int. 31-5 (1998) 245-256.

[20] J. Jiang, F. H. Stott, M. M. Stack “Characterization of wear scar surfaces using combined three-dimensional topographic analysis and contact resistance measurements” Trib. Int. 30-7 (1997) 517-526.

[21] J. Jiang, F. H. Stott, M. M. Stack “A mathematical model for sliding wear of metals at elevated temperatures” Wear 181-183 (1995) 20-31.

[22] J. Jiang, F. H. Stott, M. M. Stack “Some frictional features associated with the sliding wear of the Ni-base alloy N80A at temperatures to 250°C” Wear 176 (1994) 185-194.

[23] I.A. Inman, S.R. Rose, P.K. Datta “Studies of High Temperature Sliding Wear of Metallic Dissimilar Interfaces II: Incoloy MA956 versus Stellite 6”, Tribology International 39 (2006) 1361–1375.

[24] I.A. Inman, P.S. Datta “Development of a Simple ‘Temperature versus Sliding Speed’ Wear Map for the Sliding Wear Behaviour of Dissimilar Metallic Interfaces II” Wear 265 (2008) 1592–1605.

[25] I.A. Inman, P.K. Datta “Studies of High Temperature Sliding Wear of Metallic Dissimilar Interfaces III: Incoloy MA956 versus Incoloy 800HT”, Tribology International 43 (2010) 2051–2071.

[26] H. So “Wear Behaviours of Laser-Clad Stellite Alloy 6”, Wear 192 (1996) 78-84.

[27] H. So “Characteristics of Wear Results Tested by Pin-on-Disc at Moderate to High Speeds”, Tribo. Int., Vol. 25, No. 5 (1996) 415-423.

[28] N.C. Welsh “The Dry Wear of Steels 2, Interpretation and Special Features” Phil. Trans., 257A (1965) 51-70.

[29] N.C. Welsh “The Dry Wear of Steels 1, the General Pattern of Behaviour” Phil. Trans., 257A (1965) 31-50.

[30] J.K. Lancaster “The Formation of Surface Films at the Transition Between Mild and Severe Metallic Wear”, Proc. Royal Society London, A 273 (1962) 466-483.

[31] C. Subramanium “Wear of Al-12.3 Wt% Si Alloy Slid Against Various Counterface Materials” Scripta Metallurgica 25 (1991) 1369-1374.

[32] P.J. Blau “Mechanisms for Traditional Friction and Wear Behaviour of Sliding Metals” Wear 72 (1981) 55-66.

[33] P.D. Wood, H.E. Evans, C.B. Ponton “Investigation into The Wear Films Formed on Certain Superalloys between 20 and 600°C during Rotation in an Unlubricated Bearing” Proc. ASME/STLE Int. Joint Tribo. Conf. 2009 (Oct. 19-21, 2009) Memphis, Tennessee, USA.

[34] T.H.C. Childs “The Sliding Wear Mechanisms of Metals, Mainly Steels”, Tribo. Int. 13 (1980) 285-293.

[35] S.C. Lim “Recent Development in Wear Maps”, Tribo. Int. 31, Nos. 1-3 (1998) 87-97.

[36] S.C. Lim “The relevance of wear-mechanism maps to mild-oxidational wear”, Tribo. Int. 35, No. 11 (2002) 717-723.

[37] A. R. Riahi and A. T. Alpas – "Wear map for grey cast Fe" Wear 255 (2003) 401-409.

[38] H. Chen and A. T. Alpas – "Sliding wear map for the magnesium alloy Mg-9Al-0.9 Zn (AZ91)" Wear 246 (2000) 106-116.

[39] S.H. Yang, H. Kong, E-S. Yoon and D.E. Kim – "A wear map of bearing steel lubricated by silver films" Wear 255 (2003) 883-892.

[40] D. Grimanelis and T.S. Eyre “Wear characteristics of a diffusion bonded sintered steel with short term surface treatments” Wear 262 (2007) 93-103.

[41] D. Grimanelis and T.S. Eyre – "Sliding wear mapping of an ion nitrocarburized low alloy sintered steel" Surf. & Coat. Tech. 201-6 (2006) 3260-3268.

[42] K. Elleuch, R. Elleuch, R. Mnif, V. Fridrici and P. Kapsa – "Sliding wear transition for the CW614 brass alloy" Tribo. Int. 39-4 (2006) 290-296.

[43] S. Anbuselvan and S. Ramanathan – "Dry sliding wear behavior of as-cast ZE41A magnesium alloy" Materials & Design 31-4 (2010) 1930-1936.

[44] T. Gómez-del Río, A. Rico, M.A. Garrido, P. Poza and J. Rodríguez – "Temperature and velocity transitions in dry sliding wear of Al–Li/SiC composites" Wear 268, Issues 5-6 (2010) 700-707.

[45] K. Adachi, K. Kato and N. Chen "Wear map of ceramics" Wear 203-204 (1997) 291-301.

[46] K. Kato and K. Hokkirigawa “Abrasive Wear Diagram”, Proc. Eurotrib ’85, Vol. 4, Section 5.3, Elsevier, Amsterdam (1985) 1-5.

[47] P. Crook and C.C. Li “The Elevated Temperature Metal-to-Metal Wear Behaviour of Selected Hard Facing Alloys” Wear of Materials, ASME Publication 110254, (1983) 272-279.

[48] D.H.E. Persson "Laser processed low friction surfaces", Licentiate of Philosophy Dissertation, Uppsala University (2003).

[49] D.H.E. Persson "On the Mechanisms behind the Tribological Performance of Stellites", Ph.D. Thesis, Uppsala University (2003).

[50] D.H. Buckley “Adhesion, Friction and Wear of Cobalt and Cobalt-Base Alloys” Cobalt 38 (1968) 20-28.

[51] F.H. Stott, C.W. Stevenson and G.C. Wood – “Friction and Wear Properties of Stellite 31 at Temperatures from 293 to 1074K” Metals Tech., 4 (1977) 66-74.

[52] V. John "Introduction to engineering materials" Industrial Press (1992).

[53] G.T. Murray "Introduction to engineering materials: behaviour, properties, and selection" Marcel Dekker (1993).

[54] D.A. Rigney and W.A. Glaeser “The Significance of Near Surface Microstructure in the Wear Process” Wear 46 (1978) 241-250.

[55] M. Sawa and D.A. Rigney “Sliding Behaviour of Dual Phase Steels in Vacuum and in Air”, Wear 119 (1987) 369-390.

[56] P. Heilmann, J. Don, T.C. Sun, D.A. Rigney, W.A. Glaeser “Sliding Wear and Transfer”, Wear 91 (1983) 171-190.

[57] M. Bartsch, A. Wasilkowska, A. Czyrska-Filemonowicz and U. Messerschmidt “Dislocation Dynamics in the Oxide Dispersion Strengthened Alloy Incoloy MA956”, Mat. Sci. Eng., A272 (1999) 152-162.

[58] “INCOLOY® alloy 800H & 800HT®” Publication Number SMC-047, Special Metals (Wiggins) Ltd. (2004).

[59] N.P. Suh “The Delamination Theory of Wear” Wear 25 (1973) 111-124.

[60] H. Chandler “Heat treater's guide: practices and procedures for nonferrous alloys” ASM International (1996).

[61] T.F.J. Quinn “Review of Oxidational Wear. Part 1: The Origins of Oxidational Wear” Tribo. Int., 16 (1983) 257-270.

[62] H. So, H.M. Chen and L.W. Chen "Extrusion wear and transition of wear mechanisms of steel" Wear 265 (2008) 1142-1148.

[63] P.D.Wood, H.E.Evans, C.B.Ponton "Investigation into the Wear Behavior of Tribaloy 400C during Rotation as an Unlubricated Bearing at 600°C from 2 Minutes to 12 Hours", Wear 269 (2010) 763–769.

[64] P.D.Wood, H.E.Evans, C.B.Ponton " Investigation into the Wear Behaviour of Stellite 6 during Rotation as an Unlubricated Bearing at 600°C", to be published in Tribology International.

[65] I.A. Inman, P.S. Datta, H.L. Du, C. Kübel, P.D. Wood “High Temperature Tribocorrosion”, in: T. Richardson, B. Cottis, R. Lindsay, S. Lyon, D. Scantlebury, H. Stott, M. Graham (Eds.), Shreir's Corrosion – VOL 1: Types of High Temperature Corrosion, Elsevier Ltd (2010).

[66] J.Yoshihisa, F.Yokoyama, T.Yamasaki, N.Ohmae, “The Tribological Characteristics of Ni-Cr Cast Alloy at 1000°C in Air”, Tribology Online, Vol. 5, No. 1, (2010) 27-32.

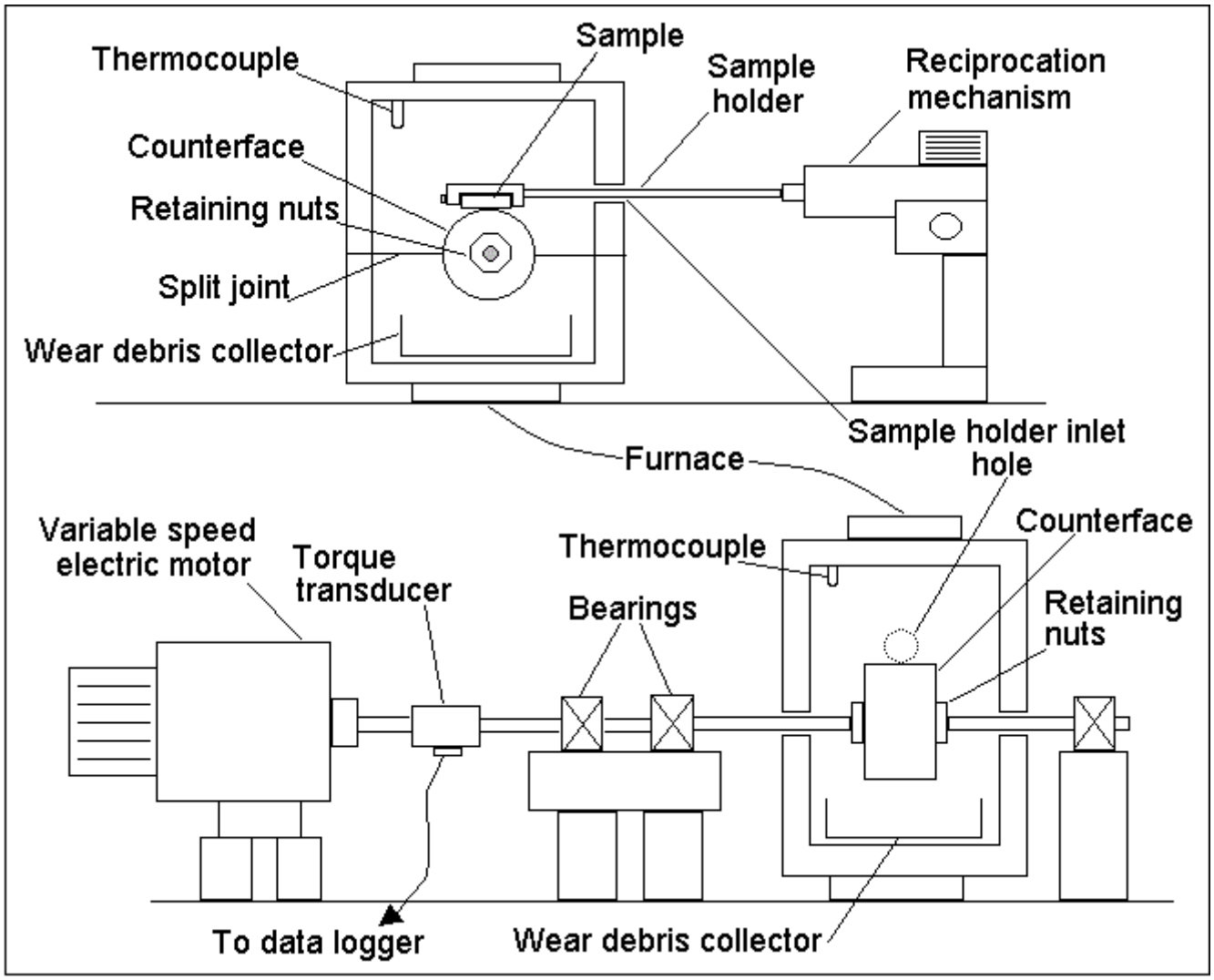

Fig. 1: Reciprocating high temperature 'block-on-cylinder' wear rig used in the current study [5]

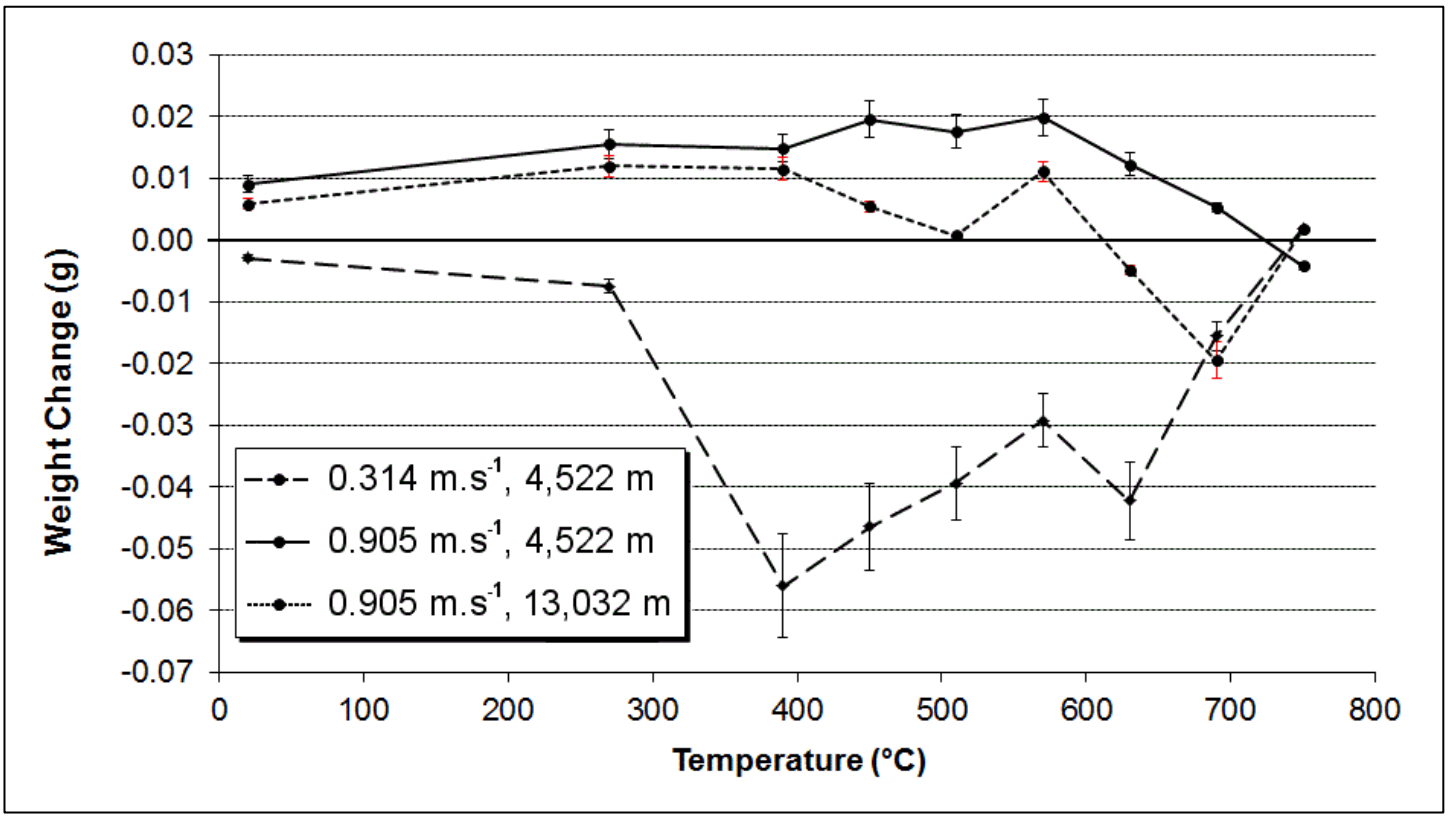

Fig. 2: Effect of temperature on weight change – Nimonic 80A vs. Incoloy 800HT
(load = 7N, sliding distance = 4,522 m, sample size = 3)

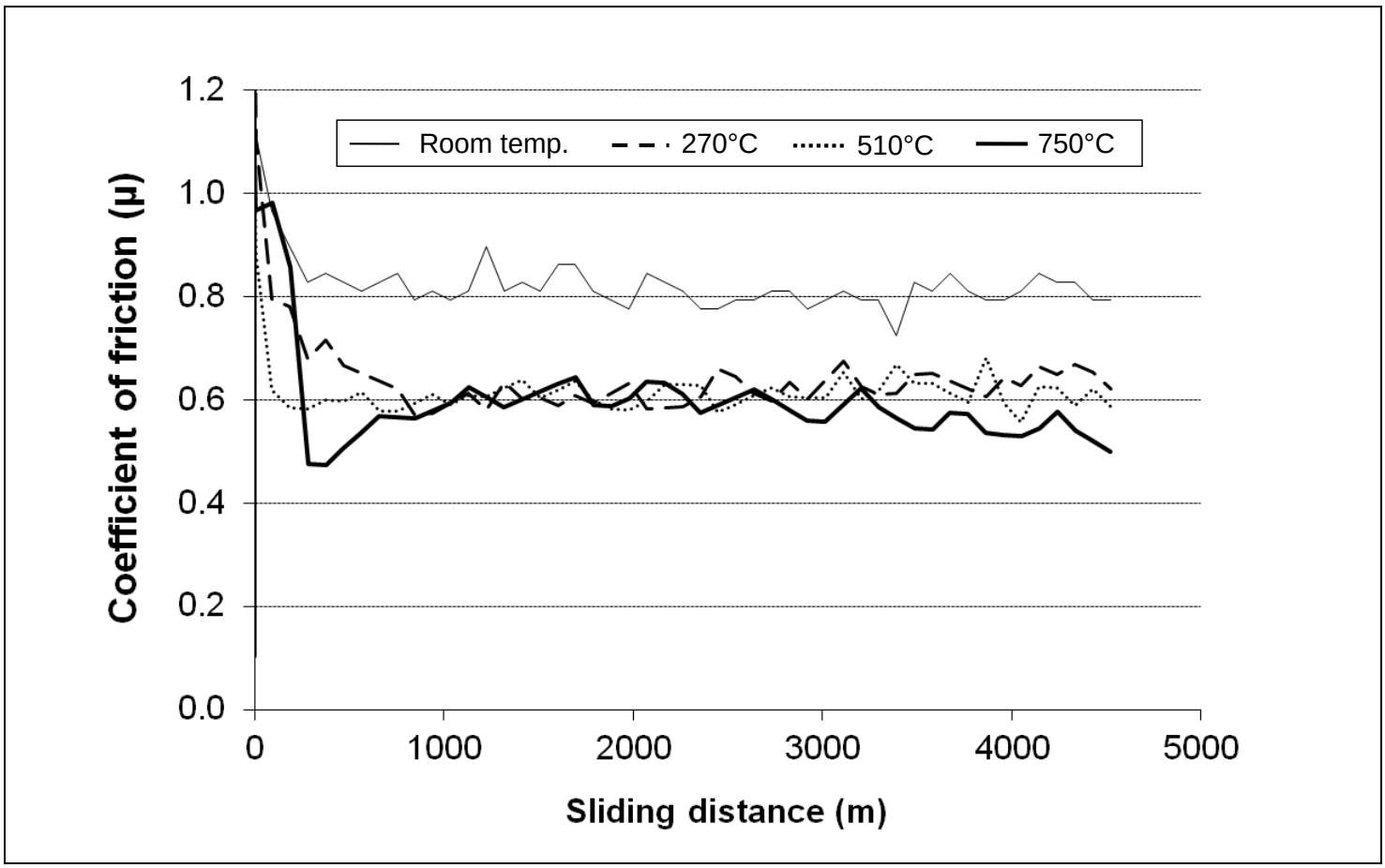

a) 0.314 m.s^{-1}

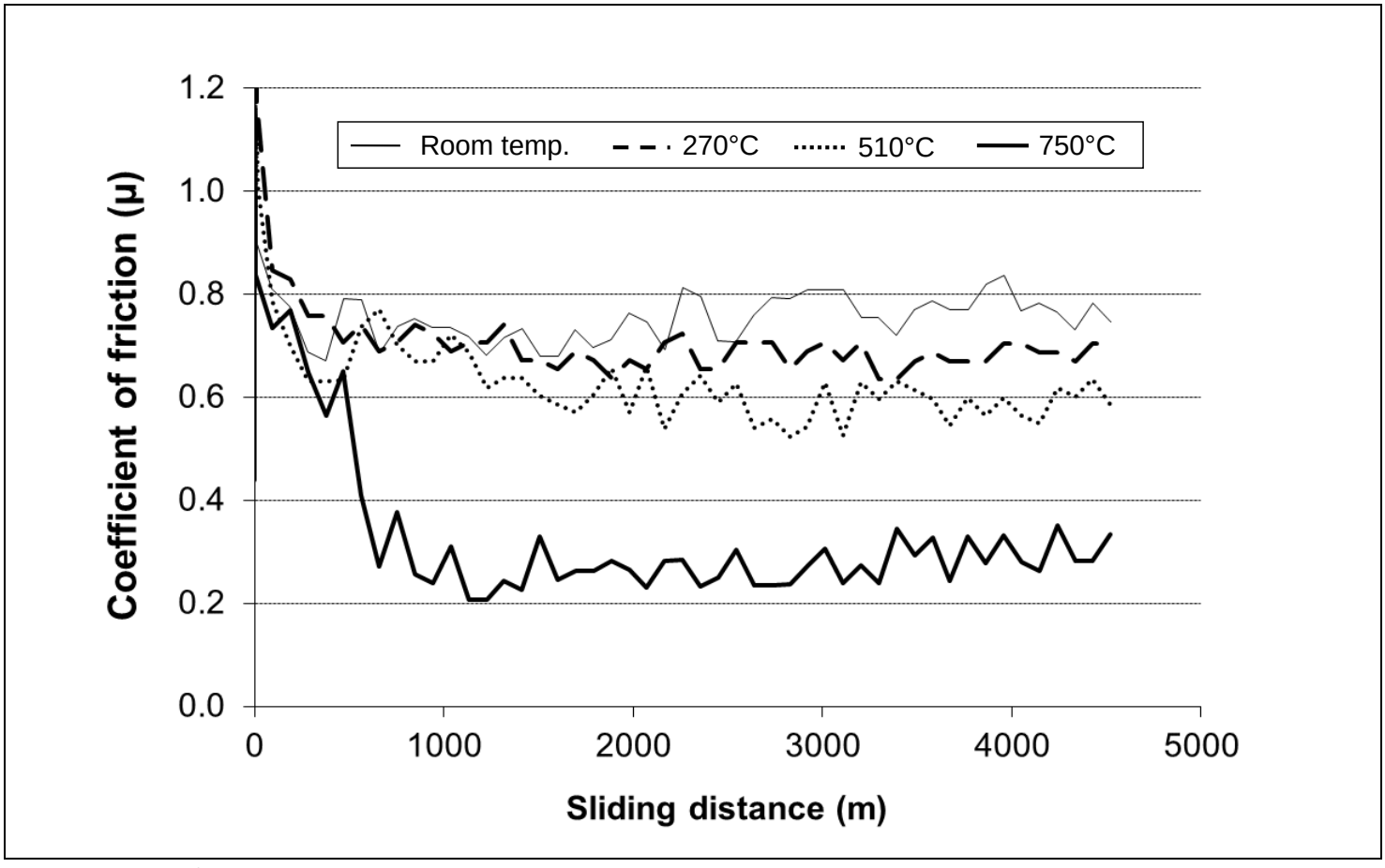

b) 0.905 m.s^{-1}

Fig. 3: Effect of temperature on friction – Nimonic 80A vs. Incoloy 800HT
(load = 7N, sliding distance = 4,522 m, sample size = 3)

	**R.T. (also 270°C), 4,522 m** *(wear scar = 15 mm, 17 mm at 270°C)* Metallic transfer layer, 90% of wear scar coverage (80% at 270°C)
	**510°C (also 390 and 450°C), 4,522 m** *(wear scar = 18 mm)* Reduced transfer (15% coverage – 35% at 390°C) in isolated patches, discolouration due to oxidation
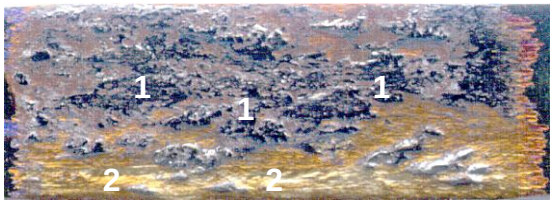	**570°C, 4,522 m** *(wear scar = 19 mm)* Patchy 'glaze' formation (1) on asperities, a few isolated areas of transferred material (2)
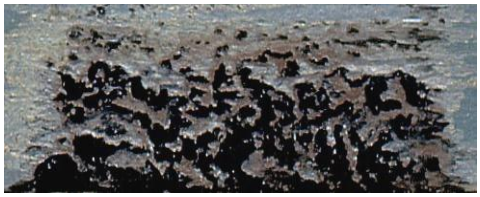	**750°C (also 630 and 690°C), 4,522 m** *(wear scar = 14 mm)* More complete 'glaze' overlying a limited amount of transferred material

(a) 0.314 m.s^{-1}

	**R.T. (also 270°C), 4,522 m** *(wear scar = 15 mm)* Metallic transfer layer covering 90% of wear scar
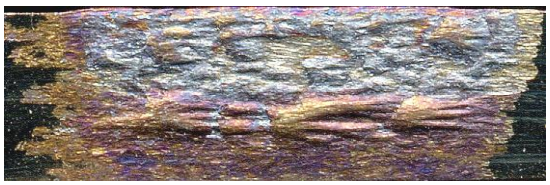	**510°C (also 390, 450 and 570°C), 4,522 m** *(wear scar = 18 mm)* Metallic transfer layer similar to R.T. – surface oxidation not inhibiting transfer
	**630°C, 4,522 m** *(wear scar = 17 mm)* Metallic transfer layer (exposed areas in troughs on surface – '1') with some patchy 'glaze' formation (2). A more complete 'glaze' layer develops after 13,032 m.
	**750°C (applicable also to 690°C), 4,522 m** *(wear scar = 14 mm)* Comprehensive 'glaze' layer overlying transferred material even after 4,522 m.

(b) 0.905 m.s^{-1}

Fig. 4: Optical Images for Nimonic 80A versus Incoloy 800HT at (a) 0.314 m.s^{-1} and (b) 0.905 m.s^{-1} *(load = 7N, sliding distance = 4,522 m)*

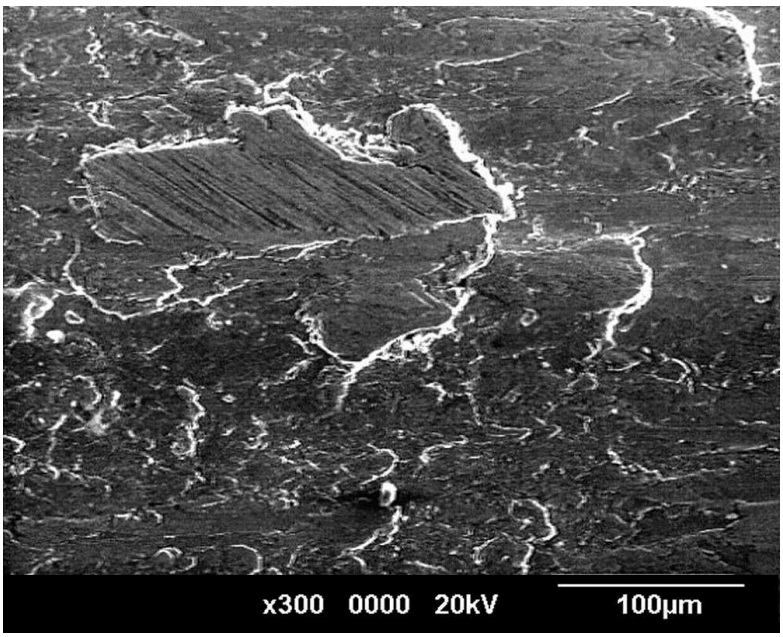

A. R.T. (shown), also 270°C

Metallic transfer layer with moderate levels of metallic debris generation

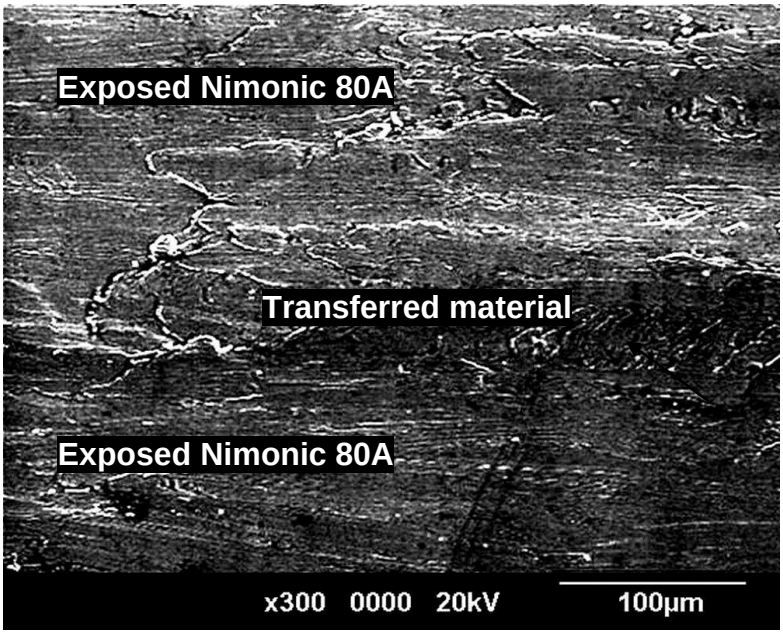

B. 510°C (shown), also 390 and 450°C

Reduced, limited patchy metallic transfer, surface mostly exposed Nimonic 80A sample material

Slight evidence of fine, parallel lines in the direction of sliding at 510°C only, a hint of oxide abrasive action in addition to the metallic wear damage

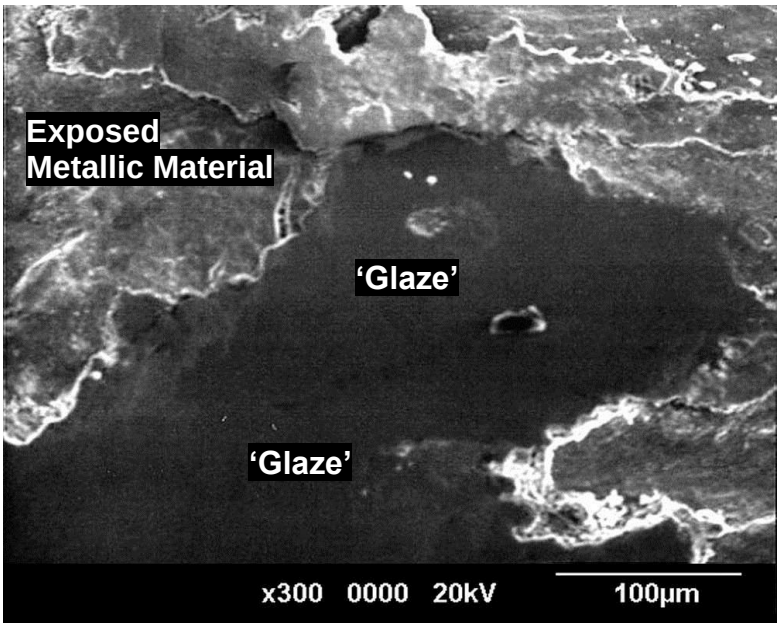

C. 750°C, also 570, 630 and 690°C

'Glaze' (greater development with increasing temperature – patchy at 570°C) overlying slightly more developed metallic transfer than seen at 510°C

Fig. 5: SEM micrographs for Nimonic 80A versus Incoloy 800HT at 0.314 $m.s^{-1}$ – wear surfaces *(load = 7N, sliding distance = 4,522 m)*

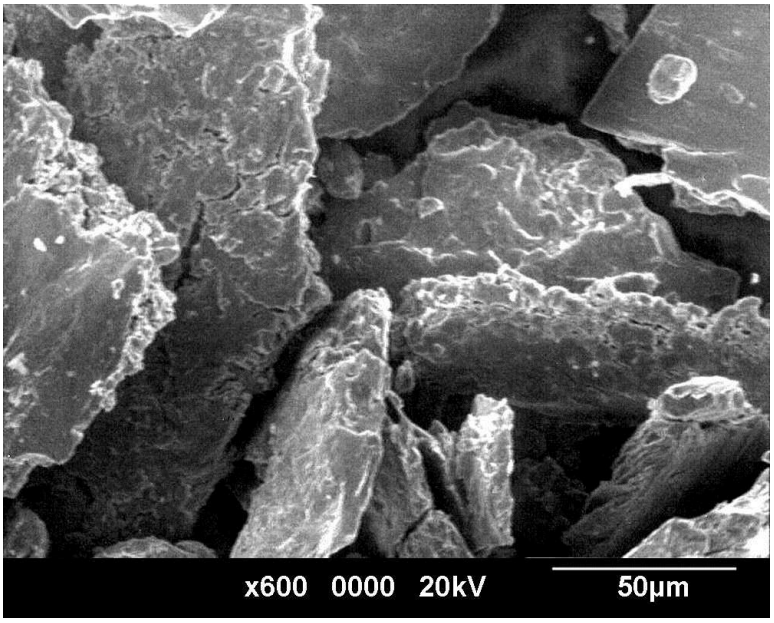

A. R.T. (shown), also 270°C

Large, flat angular metallic particles of size between 20 µm and 1 mm

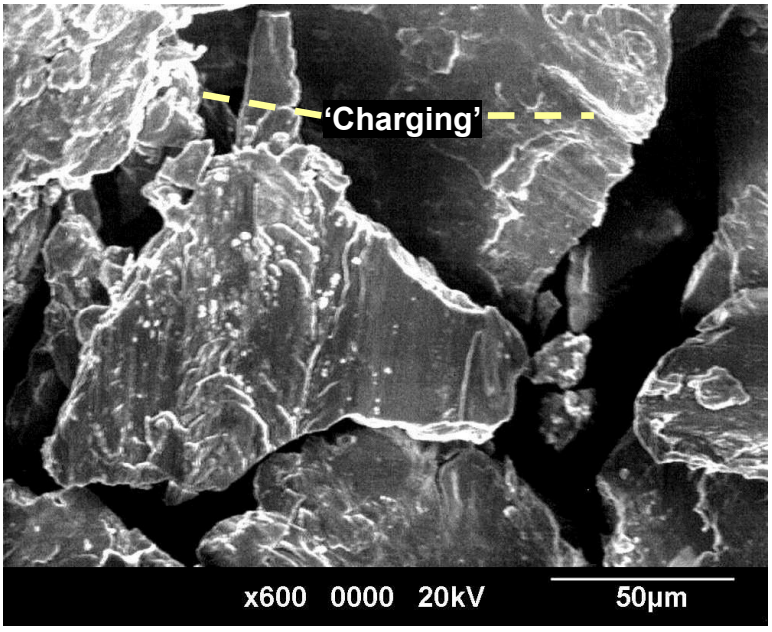

B. 510°C (shown), also 390, 450 and 570°C

Large, flat angular metallic particles of size between 20 µm and 1 mm

Very fine oxide debris (<1 µm in size) present in very low amounts from 390°C and increasing with rising temperature.

'Charging' on debris due to the presence of oxide at 510°C

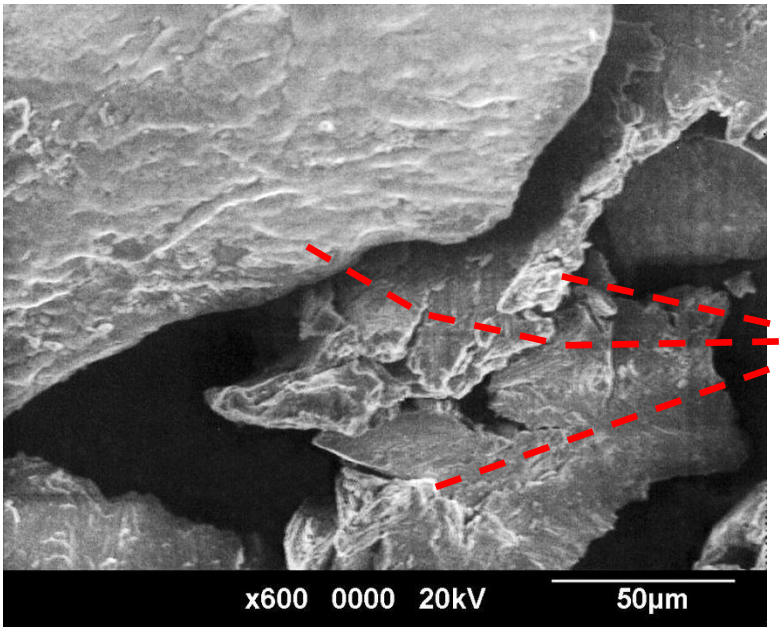

C. 750°C (shown), also 630 and 690°C

Large, flat angular metallic particles of size between 20 µm and 1 mm

Very fine oxide debris (<1 µm in size) present in increasing amounts from 630°C upwards

Fig. 6: SEM micrographs for Nimonic 80A versus Incoloy 800HT at 0.314 $m.s^{-1}$ – debris *(load = 7N, sliding distance = 4,522 m)*

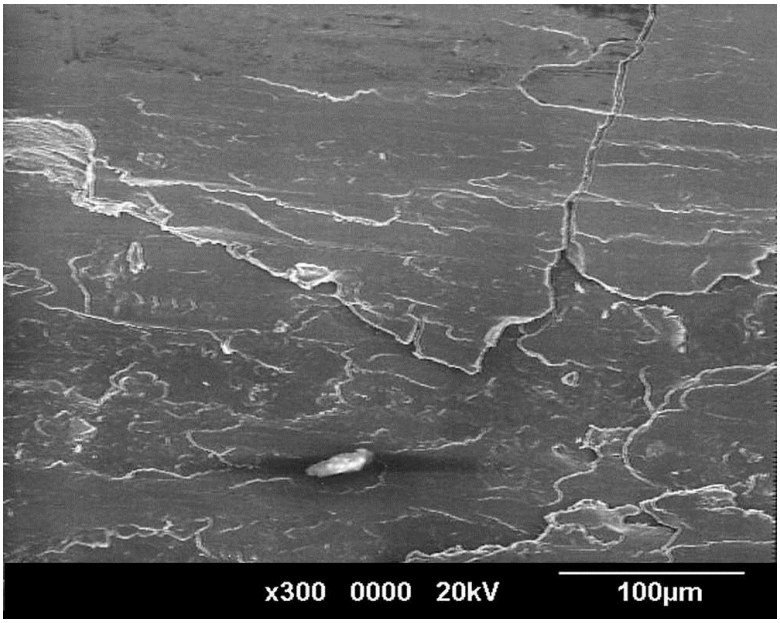	*A. R.T. (shown), also 270°C* Metallic transfer layer as observed at 0.314 $m.s^{-1}$, but greater transfer of metal onto sample surface
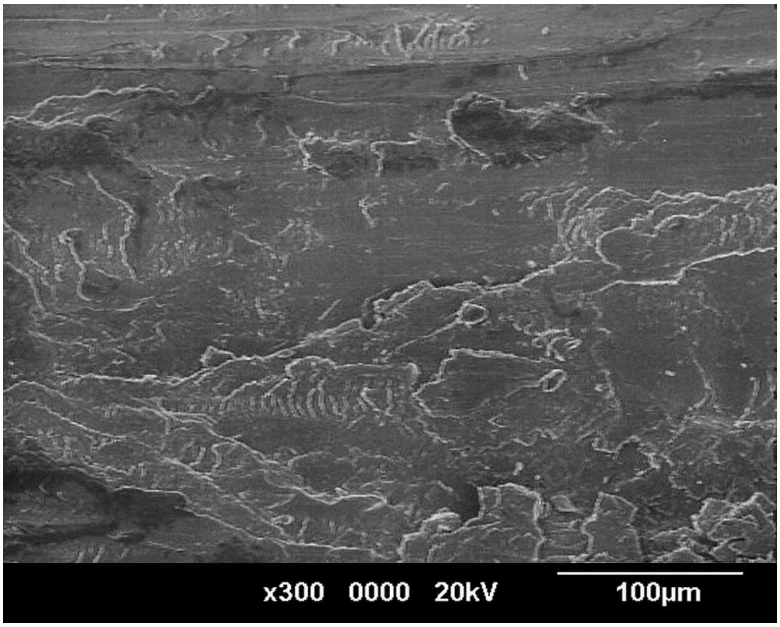	*B. 510°C (shown), also 390, 450, 570°C* Metallic transfer continuing at intermediate temperatures No evidence of oxide abrasive action at any temperature
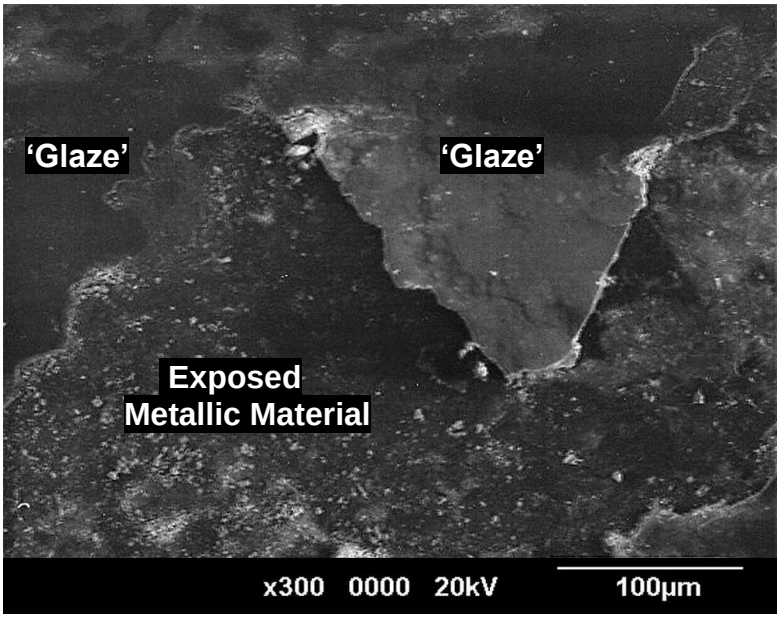	*C. 750°C (shown), also 630 and 690°C* 'Glaze' (greater development with increasing temperature) overlying limited metallic transfer layer

Fig. 7: SEM micrographs for Nimonic 80A versus Incoloy 800HT at 0.905 $m.s^{-1}$ – wear surfaces *(load = 7N, sliding distance = 4,522 m – similar observations after 13,032 m)*

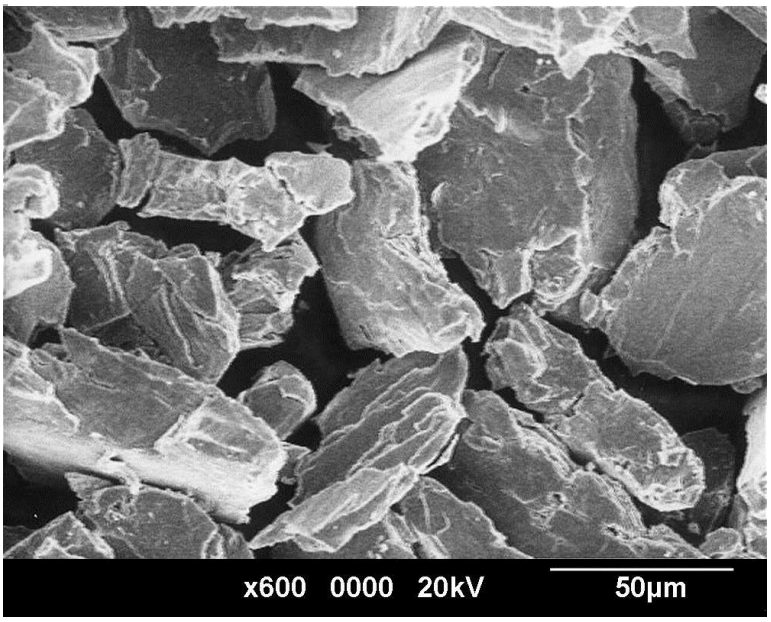

A. R.T. (shown), also 270°C

Large, flat angular metallic particles of size between 20 µm and 1 mm

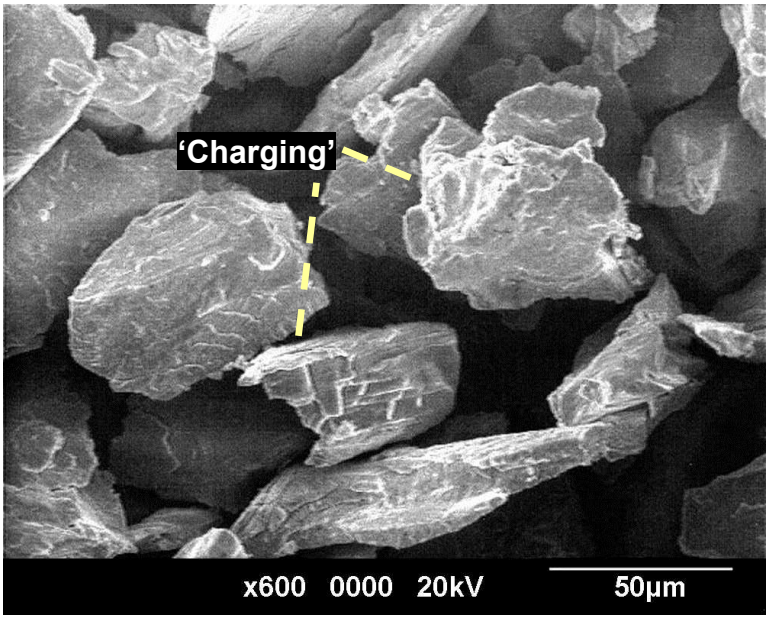

B. 510°C (shown), also 390, 450, 570 and 630°C

Large, flat angular metallic particles of size between 20 µm and 1 mm

Very fine oxide debris (<1 µm in size) present in very low amounts from 390°C and increasing with rising temperature.

'Charging' on debris due to presence of oxide at 510°C

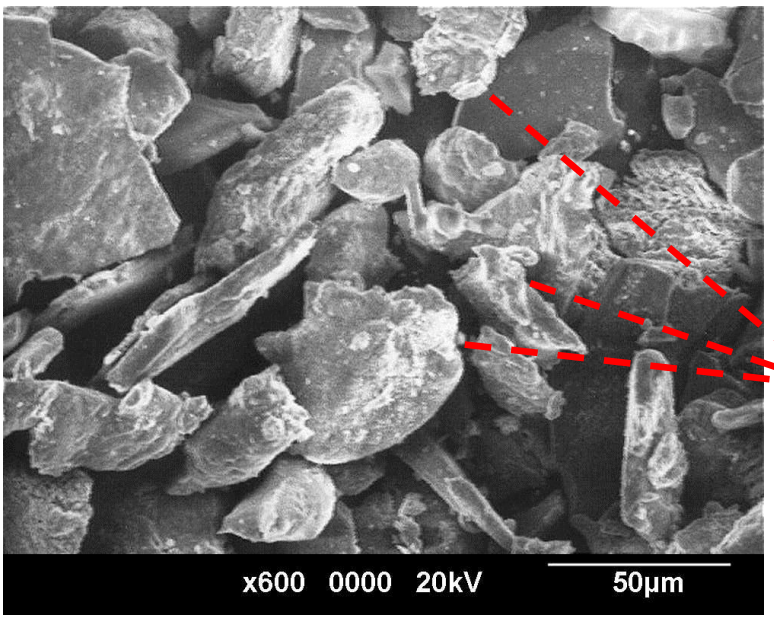

C. 750°C (shown), also 690°C

Large, flat angular metallic particles of size between 20 µm and 1 mm

Very fine oxide debris (<1 µm in size) present in increasing amounts from 630°C upwards

Fig. 8: SEM micrographs for Nimonic 80A versus Incoloy 800HT at 0.905 $m.s^{-1}$ – debris
(load = 7N, sliding distance = 4,522 m – similar observations after 13,032 m)

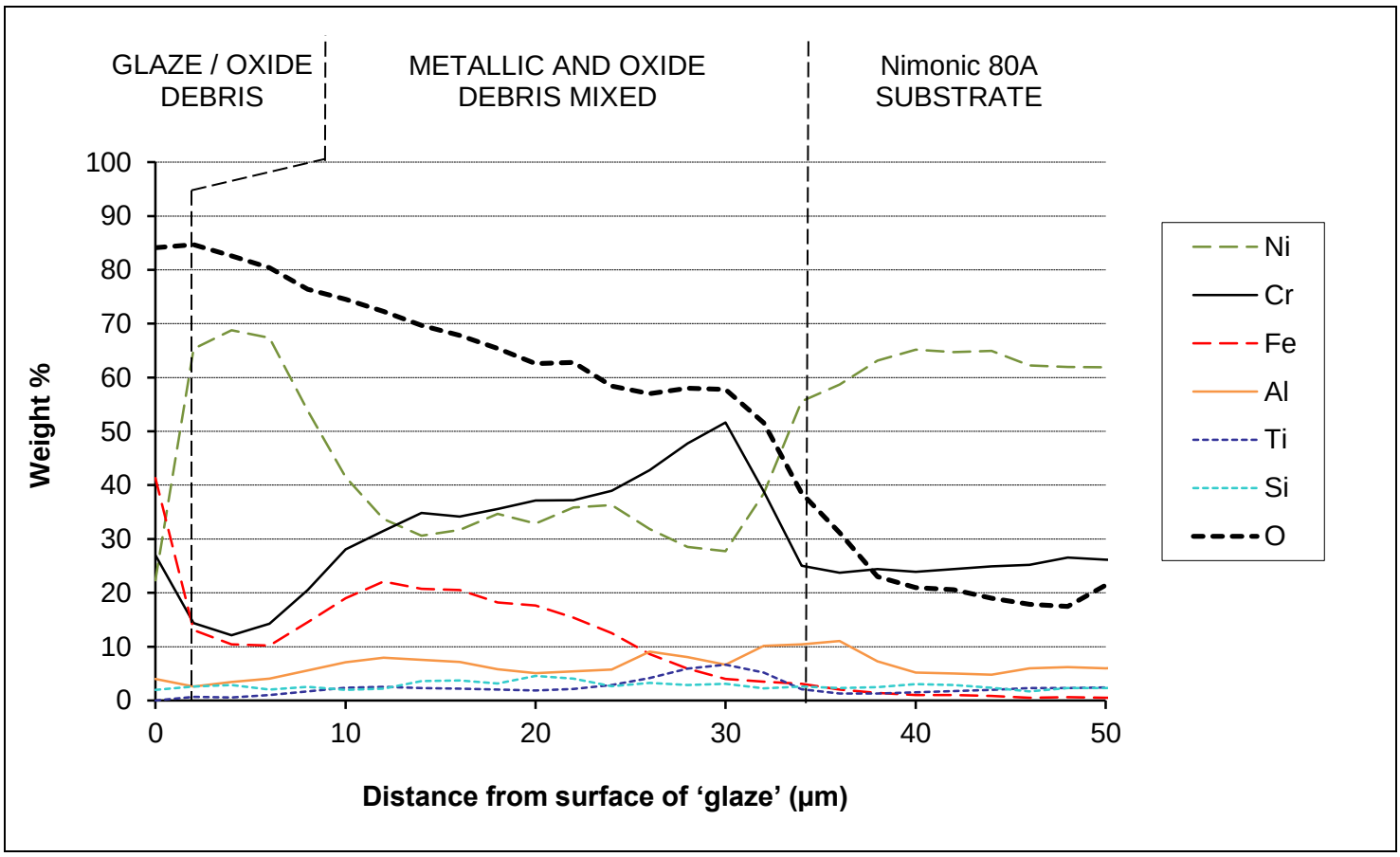

(a) Autopoint EDX

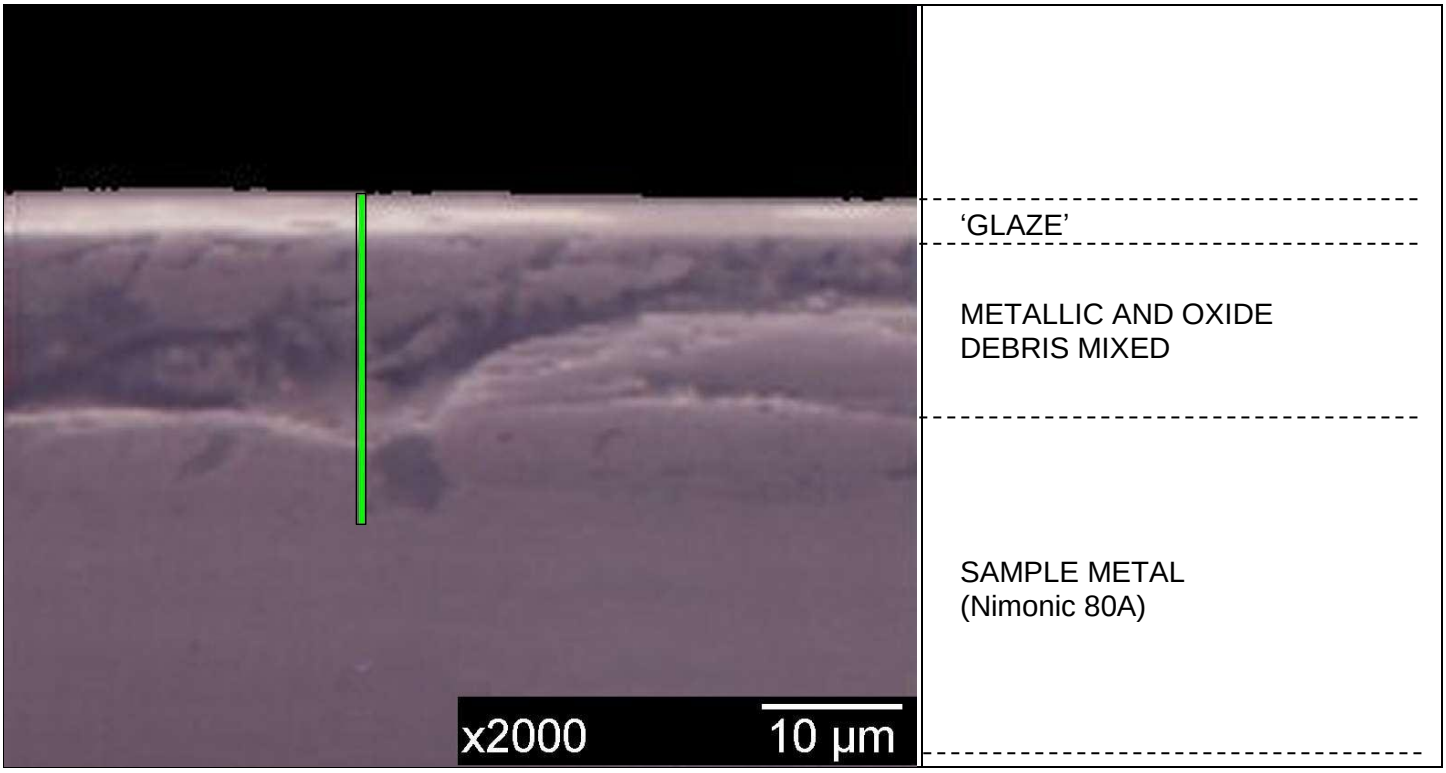

(b) Cross-section

Fig. 9: Data from Autopoint EDX analysis for Nimonic 80A versus Incoloy 800HT, sliding speed 0.314 $m.s^{-1}$, temperature 750°C (amounts of each substance present expressed as percentage of non-O content; amount of O expressed as percentage of overall content; dividing lines between different layers based on SEM observations and are average values), alongside representative cross-sections through which Autopoint EDX measurements were taken *(load = 7N, sliding distance = 4,522 m)*

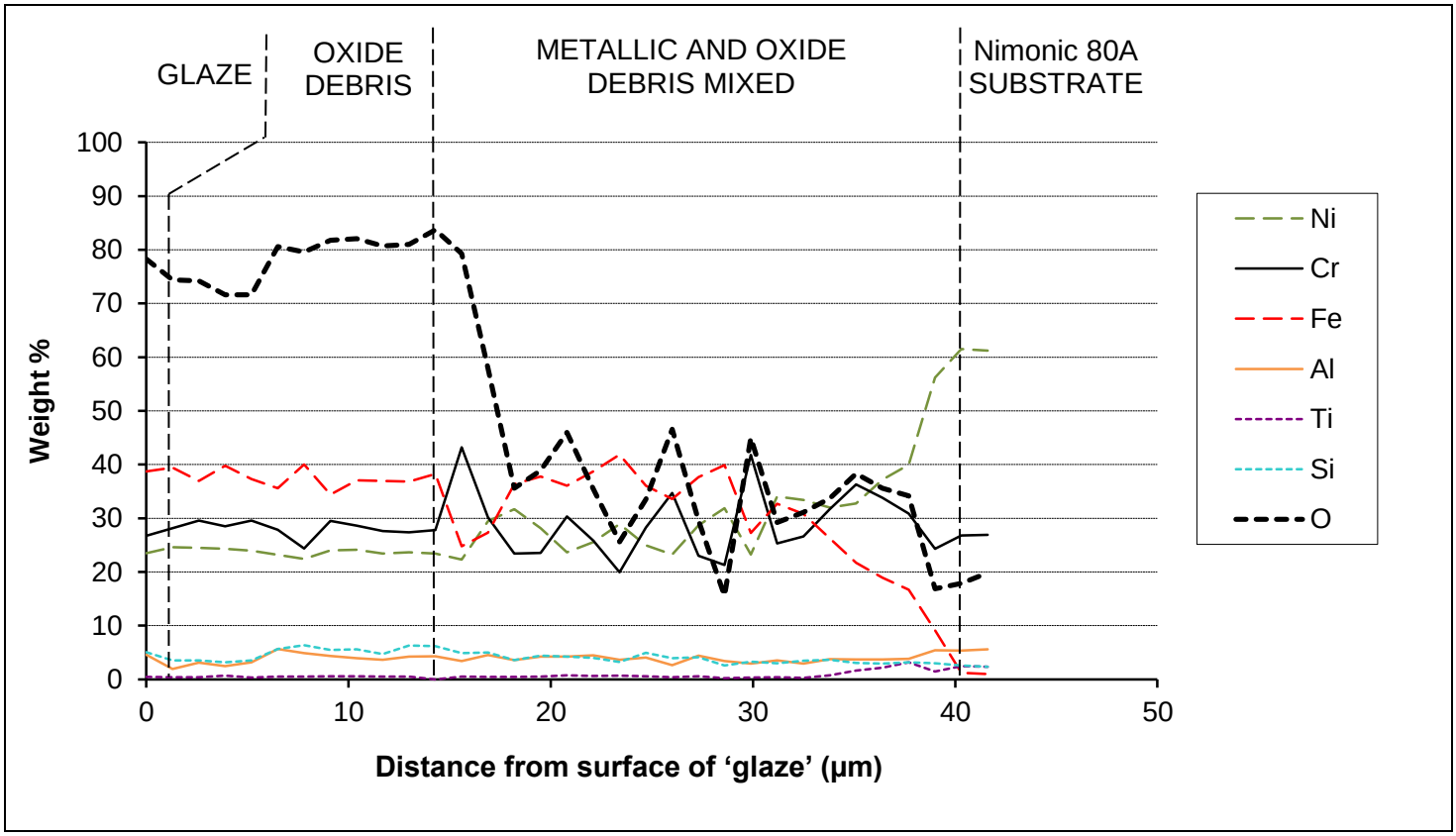

(a) Autopoint EDX

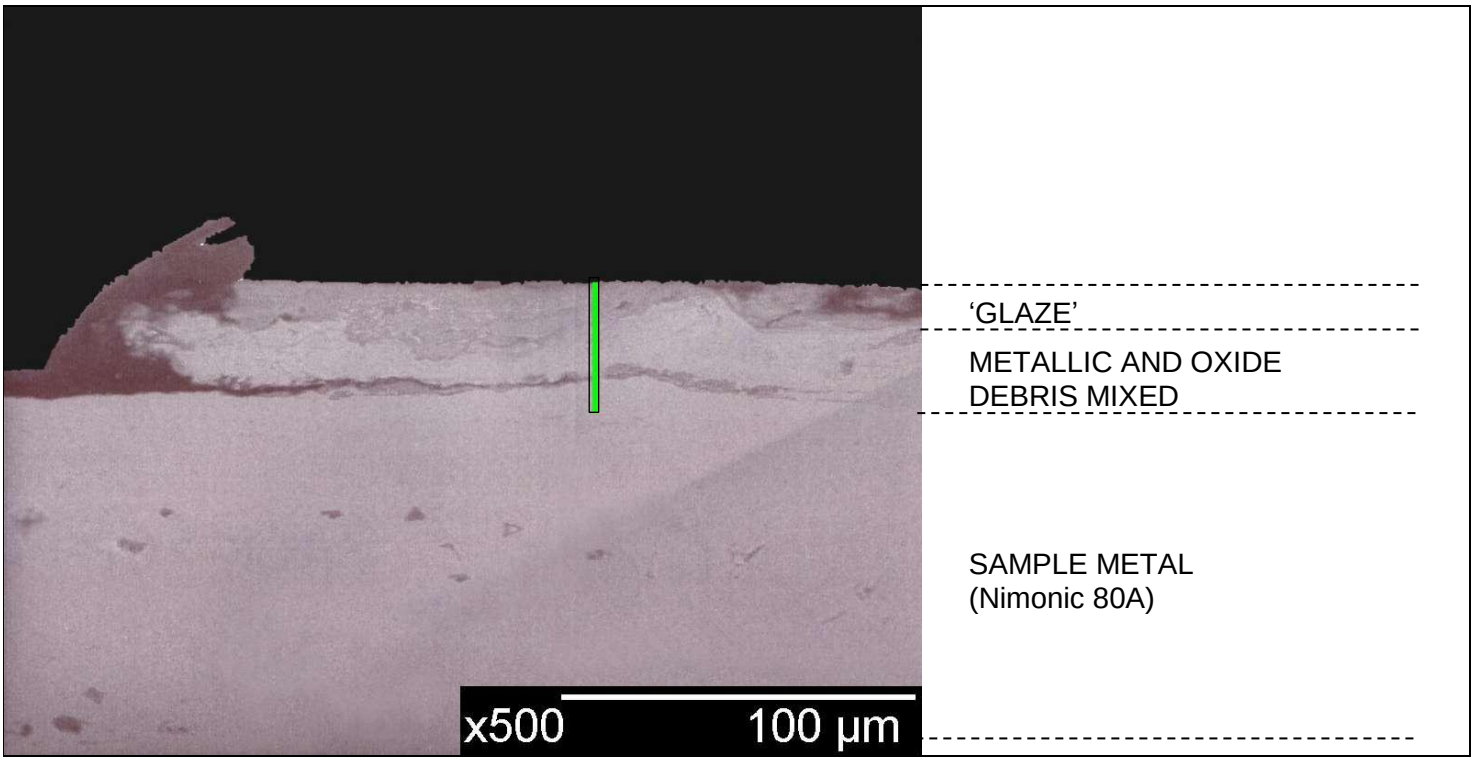

(b) Cross-section

Fig. 10: Data from Autopoint EDX analysis for Nimonic 80A versus Incoloy 800HT, sliding speed 0.905 $m.s^{-1}$, temperature 750°C (amounts of each substance present expressed as percentage of non-O content; amount of O expressed as percentage of overall content; dividing lines between different layers based on SEM observations and are average values), alongside representative cross-sections through which Autopoint EDX measurements were taken *(load = 7N, sliding distance = 4,522 m)*

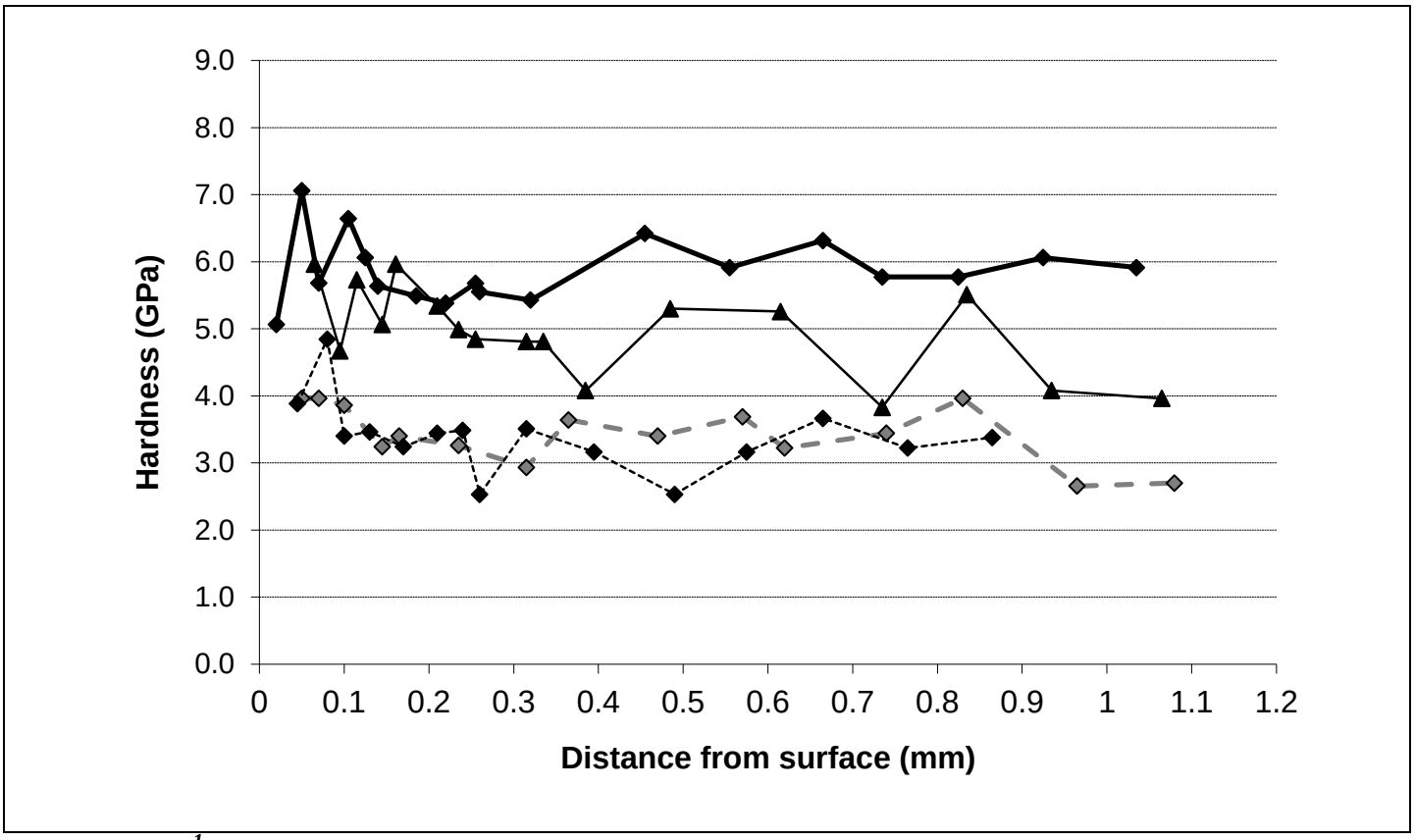

(a) 0.314 m.s^{-1}

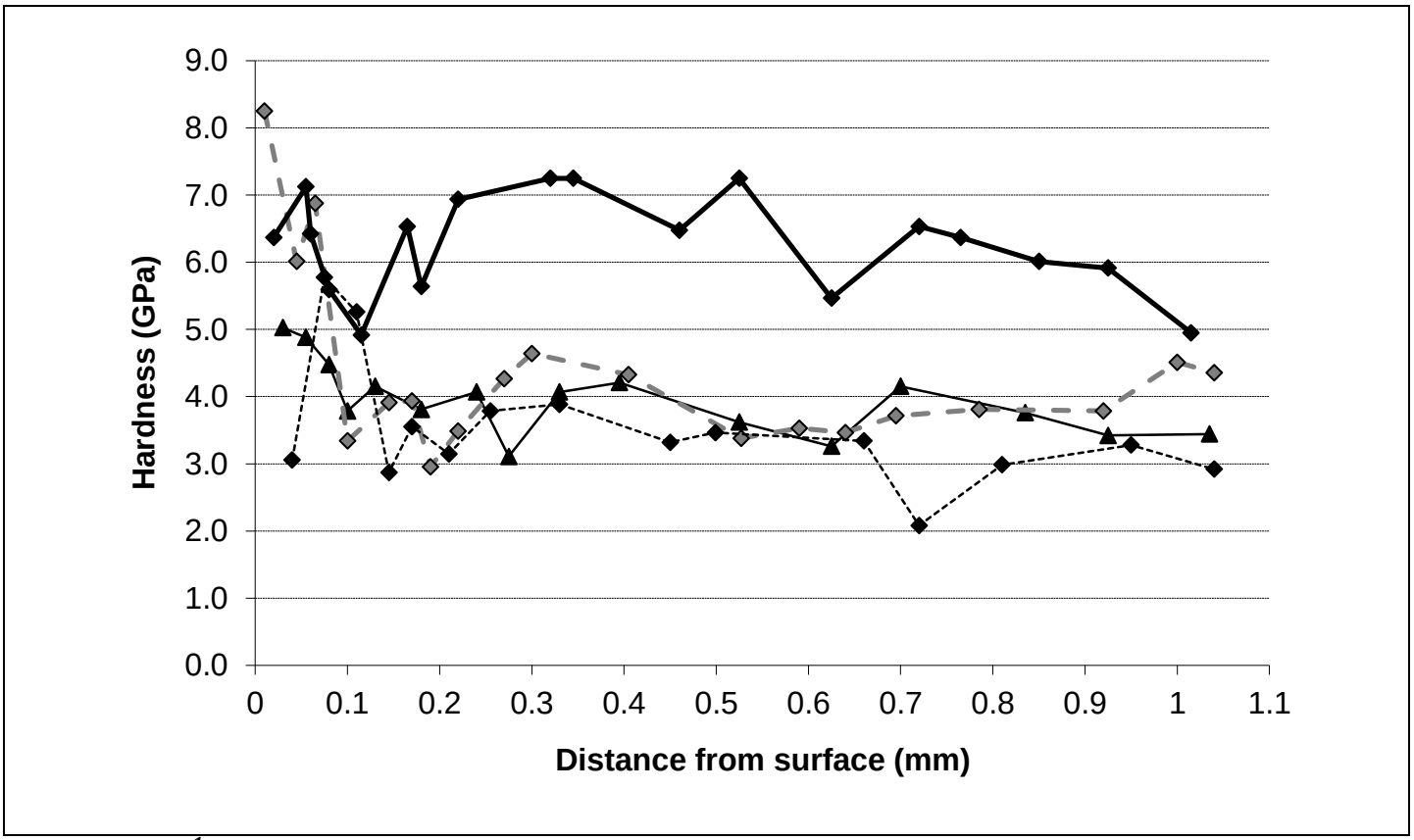

(b) 0.905 m.s^{-1}

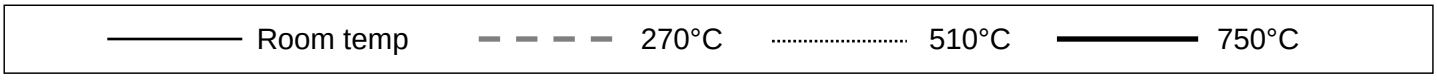

Fig. 11: Subsurface layer hardness for samples slid at 0.314 and 0.905 m.s^{-1}, Nimonic 80A versus Incoloy 800HT *(load = 7N, sliding distance = 4,522 m, hardness values in GPa, Vickers micro-indenter - 50g, sample size = 3)*

	**R.T., 4,522 m** *(section = 16 mm, representative up to 510°C)* Highly worn wear scar with limited metallic transfer
	**630°C, 4,522 m** *(section = 16 mm)* Back transferred asperities in deeply grooved wear scar, with 'glaze' on asperity peaks only
	**750°C, 4,522 m** *(section = 16 mm, applicable also to 690°C)* Back transferred asperities in deeply grooved wear scar, with 'glaze' on asperity peaks only

(a) Counterface wear scar optical images

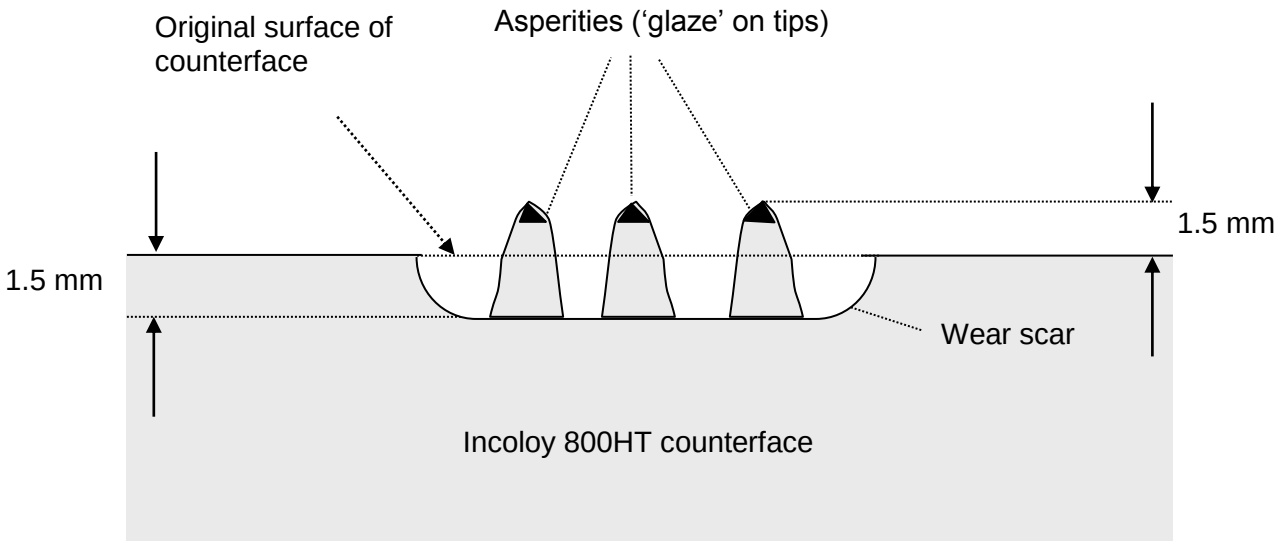

(b) Counterface wear scar cross-section schematic

Fig. 12: (a) Incoloy 800HT counterface wear scar optical images (shown optical images from 0.314 $m.s^{-1}$ after 4,522 m sliding, near-identical observations at 0.905 $m.s^{-1}$ after both 4,522 m and 13,032 m sliding); and (b) Counterface wear scar cross-section schematic for 0.314 and 0.905 $m.s^{-1}$, worn against a Nimonic 80A sample *(load = 7N)*

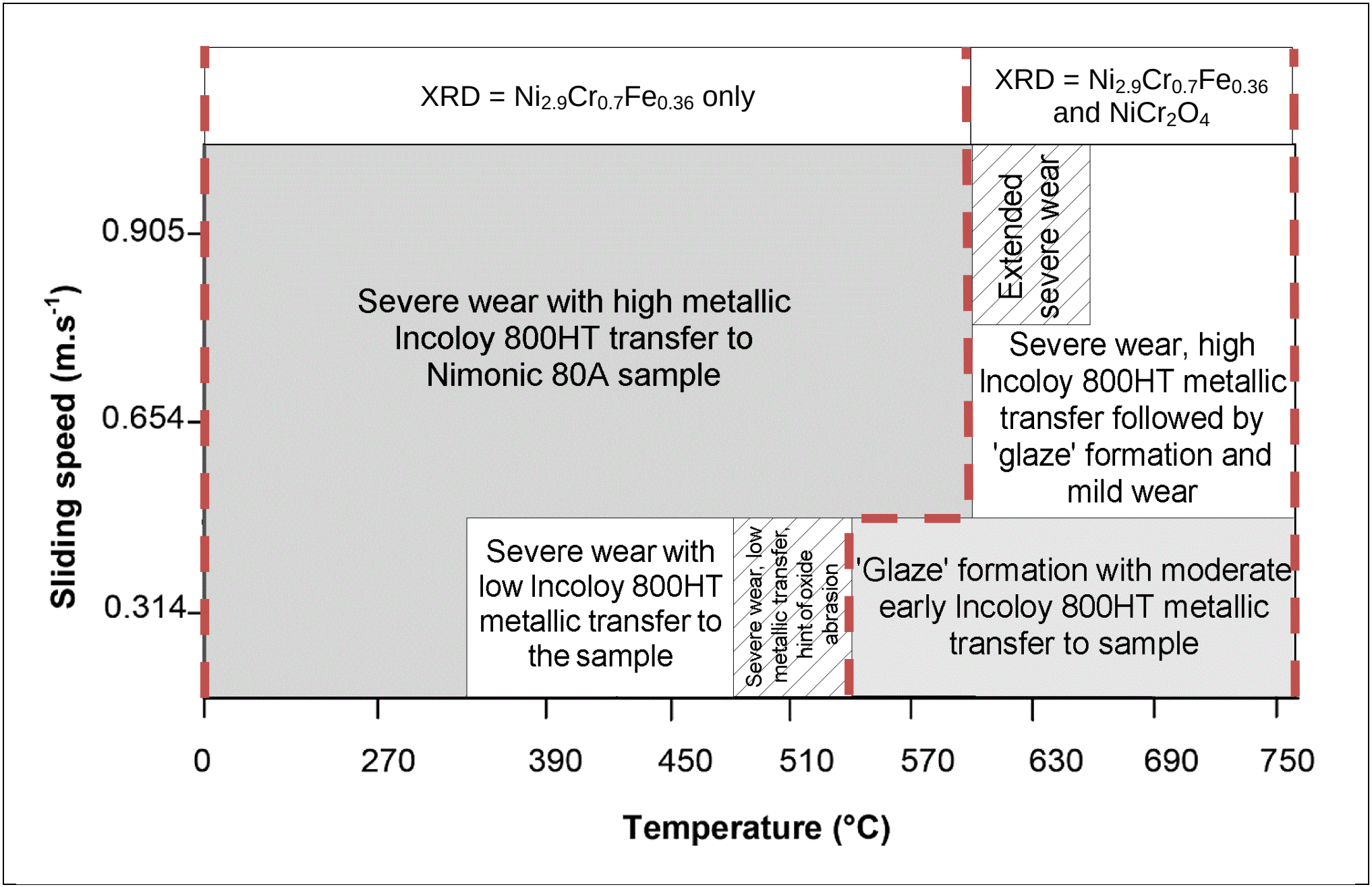

Fig. 13: Wear map for Nimonic 80A versus Incoloy 800HT between 630°C and 750°C (load = 7N); the different areas of shading denote the range of conditions over which the various detailed wear conditions were observed, also areas over which XRD results were obtained are displayed

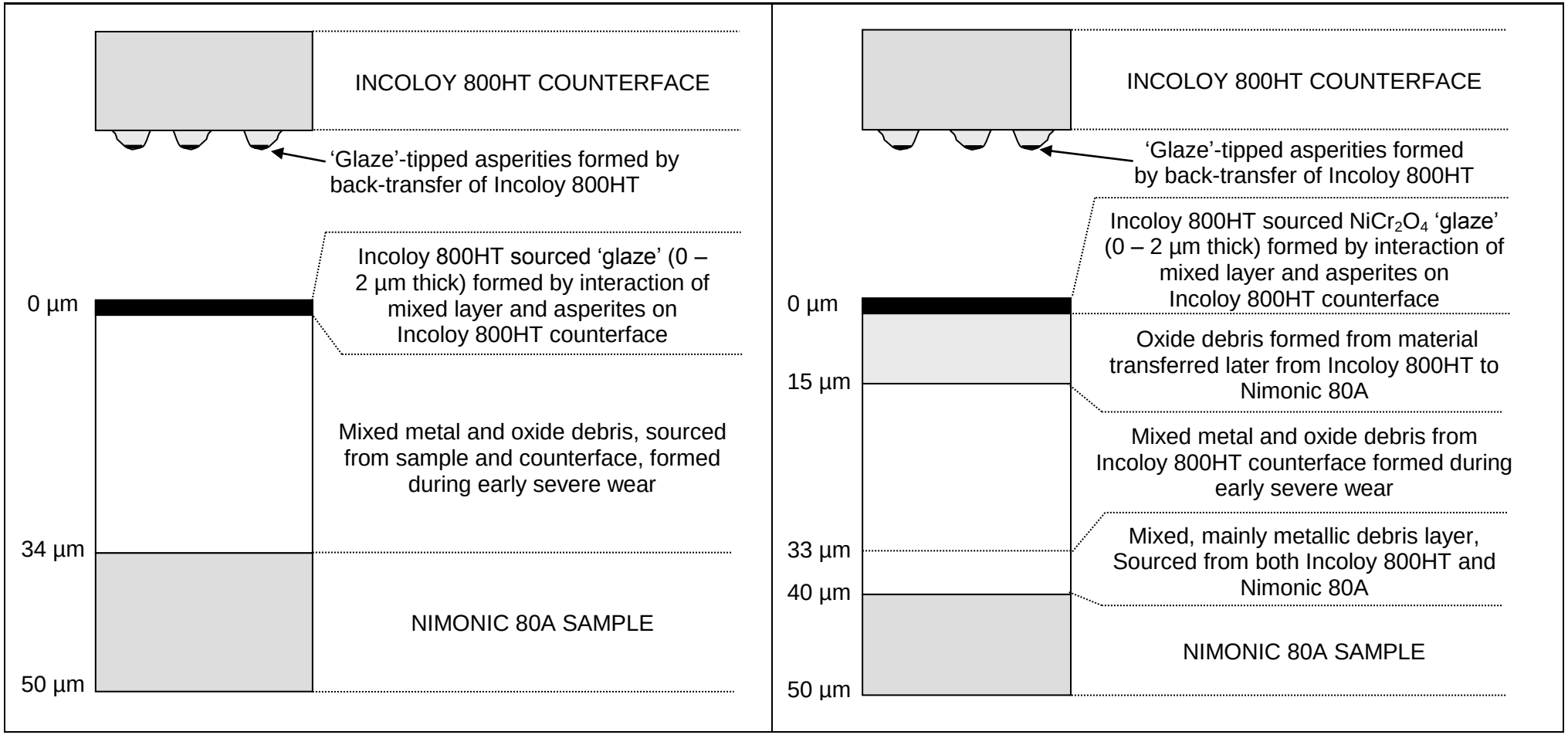

(a) 0.314 m.s^{-1} ***(b) 0.905 m.s^{-1}***

Fig. 14: Layers formed on Nimonic 80A sample and Incoloy 800HT counterface at 750°C *(load = 7N, sliding distance = 4,522 m)*

	Fe	Ni	Cr	Al	Ti	Mn	W	Co	Si	C
Nimonic 80A (specified)	0.7	75.8	19.4	1.4	2.5	-	-	-	0.1	0.08
Nimonic 80A (EDX measured)	0.75	61.54	26.56	5.79	2.33	-	-	-	2.33	(*)
Incoloy 800HT	43.8	32.5	21.0	0.37	0.37	1.5 max	-	-	0.4	0.1 max

(* - Could not measure 'C' levels using EDX.)

Table 1: Nominal compositions of alloys (wt%)

	0.314 m.s^{-1}	**0.905 m.s^{-1}**
Room temp.	5.29 ± 0.44 GPa	5.62 ± 0.55 GPa
270°C	4.97 ± 0.57 GPa	7.05 ± 1.23 GPa
390°C	No transfer layer formed	6.16 ± 0.29 GPa
450°C		6.16 ±0.49 GPa
510°C		6.18 ± 1.16 GPa
570°C		6.69 ± 0.41 GPa
'Glaze' layers at 750°C	19.97 ± 6.06 GPa	18.06 ± 7.20 GPa

(Mean hardness of unworn Nimonic 80A (sample) = 5.23 GPa;
mean hardness of unworn Incoloy 800HT (counterface) = 2.15 GPa;
hardness measurements taken after pre-heating to 750°C for 4 hours)

Table 2: Hardness data for transfer layers between R.T. and 570°C, also 'glaze' layers at 750°C, Nimonic 80A versus Incoloy 800HT *(load = 7N, sliding distance = 4,522 m, hardness values in GPa, Vickers micro-indenter - 50g, sample size = 5)*

Temperature (°C)	**30**	**150**	**270**	**390**	**450**	**510**
Nimonic 80A	3.33	2.75	2.58	2.50	2.37	2.01
Incoloy 800HT	3.38	2.16	1.68	1.52	1.34	0.55
Incoloy MA 956	1.99	1.71	1.45	1.24	1.16	0.97

Table 3: Mean Knoop hardness (hot hardness, 50 g load, 12 s dwell time) of Nimonic 80A and Incoloy 800HT between R.T. and 510°C [6] – Incoloy MA956 data provided for comparison purposes

WITHDRAWN FROM PAPER

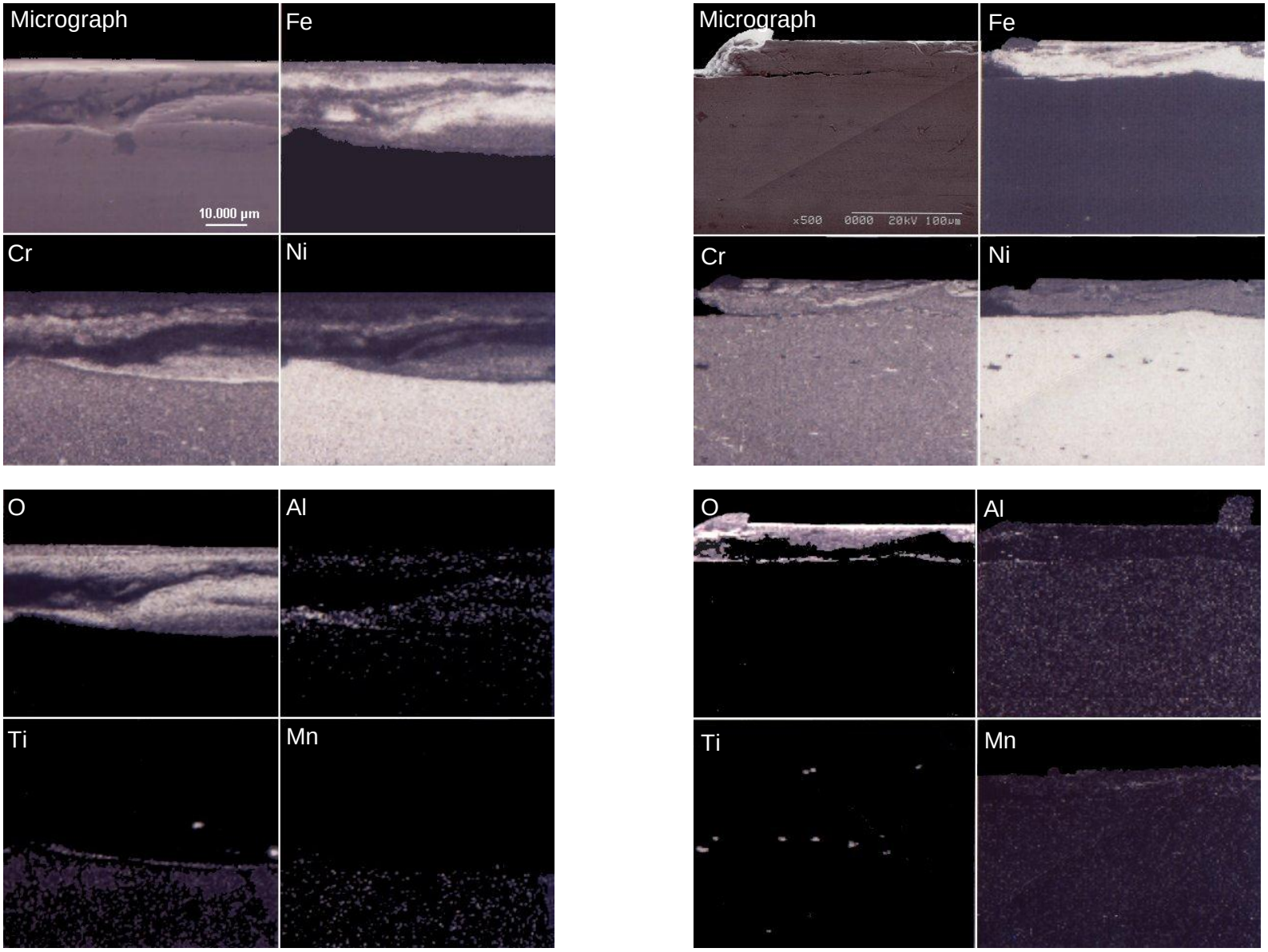

a) 0.314 m.s^{-1} ***b) 0.905 m.s^{-1}***

Fig. 15: Cross-sectional EDX element maps for Nimonic 80A worn against Incoloy 800HT subsequent to wear
(load = 7N, sliding distance = 4,522 m, temperature = 750°C, sample size = 3)